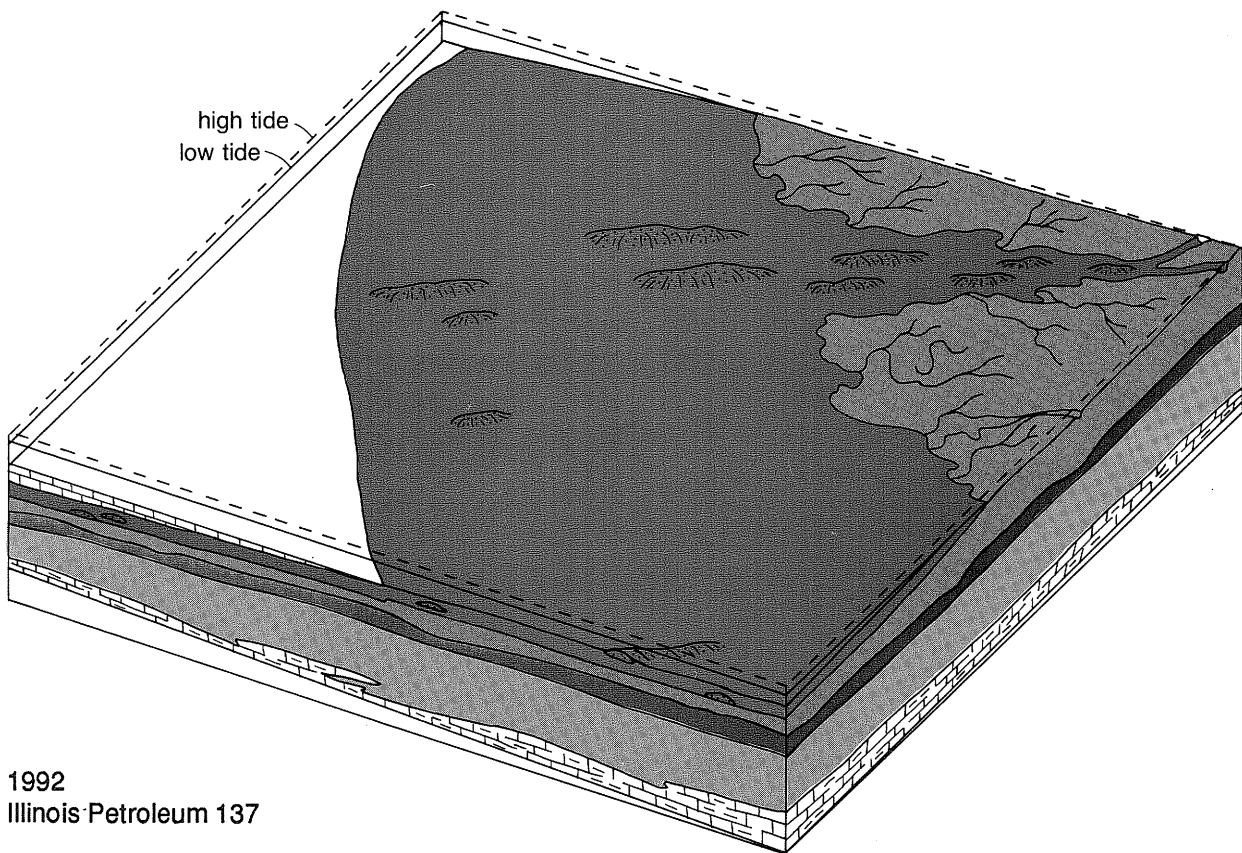


# Reservoir Heterogeneity and Potential for Improved Oil Recovery within the Cypress Formation at Bartelso Field, Clinton County, Illinois

Stephen T. Whitaker

Andrew K. Finley



1992  
Illinois Petroleum 137

Department of Energy and Natural Resources  
ILLINOIS STATE GEOLOGICAL SURVEY

# Reservoir Heterogeneity and Potential for Improved Oil Recovery within the Cypress Formation at Bartelso Field, Clinton County, Illinois

Stephen T. Whitaker

Andrew K. Finley

1992  
Illinois Petroleum 137

ILLINOIS STATE GEOLOGICAL SURVEY  
Morris W. Leighton  
Natural Resources Building  
615 East Peabody Drive  
Champaign, Illinois 61820

**Disclaimer**

This report was prepared by the Illinois State Geological Survey (ISGS) as part of a project sponsored by the State of Illinois and the U.S. Department of Energy. It presents reasonable interpretations of available scientific data. Neither the ISGS, nor any individual members of the ISGS staff, nor the U.S. Department of Energy assumes any liability with respect to the use of any information contained in this report or for damages resulting from it.

## **CONTENTS**

<b>ABSTRACT</b>	1
<b>INTRODUCTION</b>	3
<b>DISCOVERY AND PRODUCTION HISTORY</b>	4
Discovery History	4
Production History	4
<b>RESERVOIR AND TRAP CHARACTERISTICS</b>	5
Reservoir Geometry	5
Paleostructural Influence	13
Trap Type	14
Reservoir Lithofacies	14
Depositional Environment	16
Diagenesis	17
Summary	20
<b>CLASSIFICATION AND IDENTIFICATION OF PLAYS</b>	20
Delta Front	20
Upper Shoreface	20
Coastal Plain	21
Marine Bars	21
<b>PRODUCTION CHARACTERISTICS</b>	24
Drilling and Completion Practices	24
Injection and Production Data	24
Oil Characteristics	25
Water Characteristics	25
Original Volumetrics	25
<b>DEVELOPMENT AND PRODUCTION STRATEGY</b>	26
Recommendations	26
<b>ACKNOWLEDGMENTS</b>	27
<b>REFERENCES</b>	28
<b>APPENDIXES</b>	30
A Reservoir Fluid Analyses	30
B Gas Chromatograms of Saturated Hydrocarbons	38
C Reservoir Summary	39

## PLATES

- 1 Thin section from sandstone within the red interval in the No. 1 Kempwerth
- 2 Thin section from sandstone within the red interval in the No. 1 Kempwerth
- 3 SEM photomicrograph of partially dissolved feldspar grain from the red interval in the No. 1 Kempwerth
- 4 Photomicrograph of syntaxial calcite cement on echinoderm fragment from the red interval in the No. 1 Kempwerth
- 5 Photomicrograph of clay minerals interspersed with sand grains from the red interval in the No. 1 Kempwerth
- 6 Same section as in plate 5 under crossed nicols
- 7 Photomicrograph of quartz sand grains from the No. 1 Hempen
- 8 Photomicrograph of clay-mineral concentrations along a bedding plane within sandstone from the red interval in the No. 1 Kempwerth

## FIGURES

- 1 Location of Bartelso Field 3
- 2 Generalized stratigraphic column for southern Illinois 4
- 3 Structure map on the top of the Beech Creek (Barlow) Formation at Bartelso Field 6
- 4 Type log for the Cypress Formation at Bartelso Field 7
- 5 Stratigraphic cross sections 1-4 8
- 6 Isopach map of clean sandstone within the purple interval 10
- 7 Isopach map of clean sandstone within the gray interval 11
- 8 Isopach maps of clean sandstone within the red interval 12
- 9 Core analysis of (a) the red interval in the Ohio Co. No. 2 Trame well (SE NE NW, Sec. 8, T1N-R) and (b) the purple interval from the Woofter No. 1 Hempen well (SE SW NE, Sec. 10, T2N-R3W) 15
- 10 Proposed sequence stratigraphy of the Cypress and adjacent intervals at Bartelso 18
- 11 Interpreted diagenetic sequence in the Cypress sandstones at Bartelso Field 19
- 12 Depositional model for the Cypress at Bartelso Field 22
- 13 Production decline curve for Bartelso Field (Cypress and Silurian reef reservoirs commingled) 24

## TABLES

- 1 Mineral analysis of the clay-size particles 16
- 2 Analyses of Cypress oil samples from Bartelso Field 25

## ABSTRACT

The Mississippian Cypress Formation (Chesterian) is 100 feet thick at Bartelso Field and comprises a section of shales and sandstones that has produced about 2.5 million barrels of oil from 76 wells since production first began in 1936. The reservoir rocks are clean quartz arenites to subarkoses deposited under shallow marine conditions. Porosity ranges from 16% to 25%, and permeabilities range from 100 to about 500 millidarcies in the reservoir rocks.

The Cypress Formation was subdivided into four intervals, each separated by shale layers. These four intervals were arbitrarily labeled, in ascending order, pink, purple, gray, and red. On the basis of wireline log correlations, subsurface mapping, and petrographic studies of well cuttings and core samples, the authors interpreted the environments of deposition for these intervals to be as follows: (1) pink interval — shallow subtidal influences in a delta-front setting; (2) purple interval — shoreface subjected to some tidal influence; (3) gray interval — tidal flat to lagoonal influences, possibly some lower coastal plain; and (4) red interval — upper shoreface subjected to strong tidal influences. These environments indicate that the pink, purple, and gray intervals were deposited in a prograding sequence, with the gray interval representing sediments deposited under the shallowest conditions. Sandstones within the red interval represent tidal ridges (tidal bars) formed in marine conditions during a transgressive phase that inundated the deltaic complex.

Petrographic and mineralogic analyses revealed that silica is the primary cementing agent of Cypress sandstones at Bartelso. Most of the silica is in the form of quartz overgrowths, although minor amounts of chert are also present. Calcite cement is rare and is restricted to syntaxial cement around echinoderm fragments.

Clay minerals constitute less than 2% of the total rock and comprise mainly kaolinite with lesser amounts of chlorite, iron-rich chlorite, and illite. Porosity enhancement has resulted from the partial dissolution of potassium feldspars and calcium-rich plagioclases.

Reservoir compartmentalization is a factor in recovery efficiency for the sandstones of the red interval. Currently, all sandstone reservoirs in Illinois are required to be developed on a 10-acre well spacing. The shingled bars separated by thin shales that characterize the red interval preclude effective drainage with a 10-acre spacing. The less heterogeneous sandstones within the purple and gray intervals, however, may be relatively well-drained by 10-acre well spacing. Sandstones within the pink interval contained no hydrocarbons at Bartelso, but correlative units may provide reservoirs in other areas of the basin.

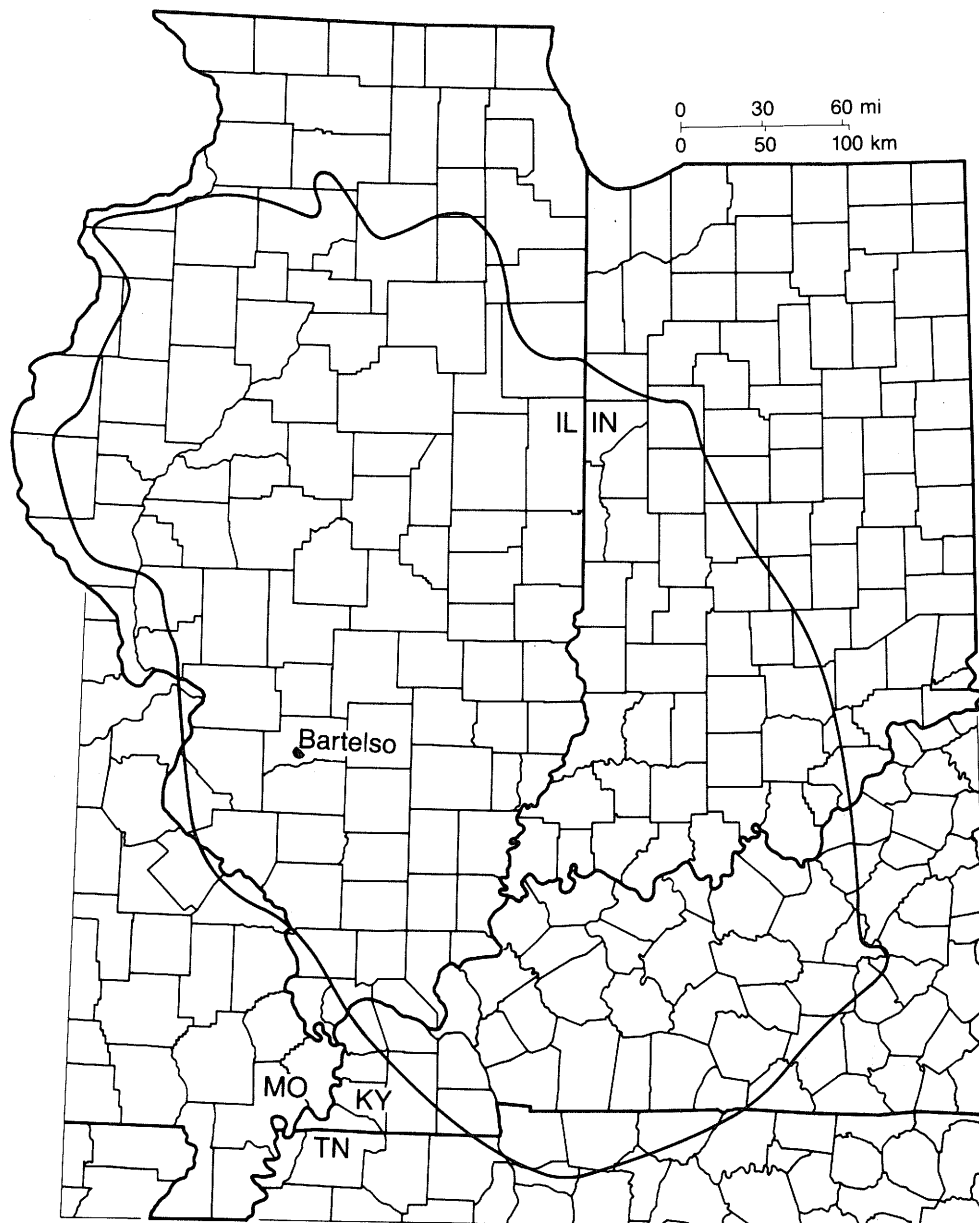


**Figure 1** Location of Bartelso Field.

## **INTRODUCTION**

Bartelso Field is located in south-central Clinton County, Illinois (Secs. 4, 5, 8, and 9, T1N-R3W), along the southwestern flank of the Illinois Basin (fig. 1). The area contains several oil fields of small to medium size, and is characterized by a relatively thick (100 to 200 ft) mantle of glacial till and soil exhibiting little topographic relief.

The goals of this study of the Cypress Formation at Bartelso Field (fig. 2) were to (1) determine the environment of deposition for each of the Cypress reservoirs, (2) determine how the depositional environment relates to reservoir heterogeneity, (3) describe how reservoir heterogeneity affects recovery efficiency, (4) estimate remaining oil in place, (5) discuss the effectiveness of the recovery methods used in the field, and (6) discuss any other recovery methods that might improve the recovery efficiency.

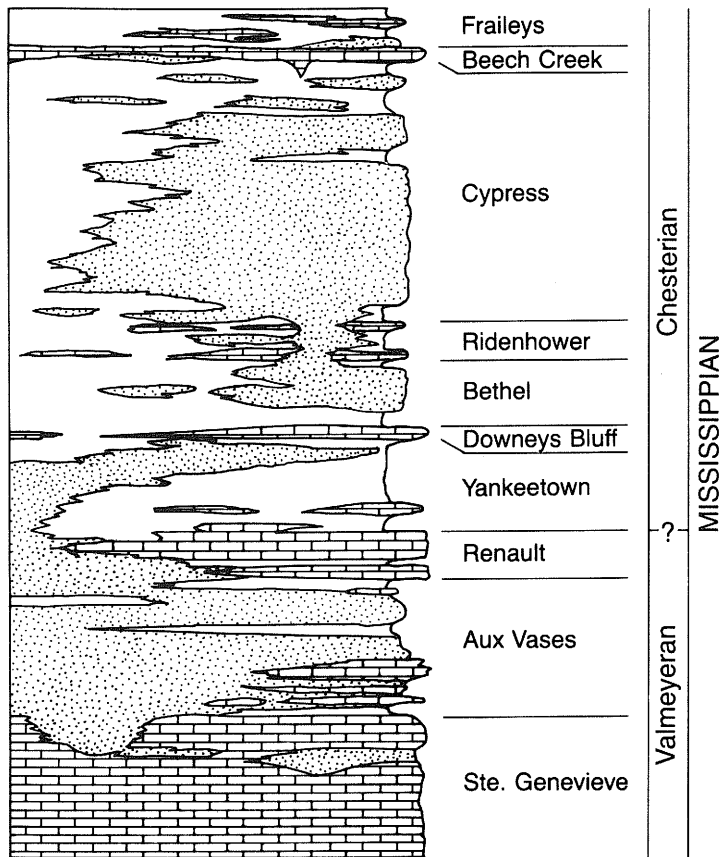


**Figure 2** Generalized stratigraphic column for southern Illinois.

## DISCOVERY AND PRODUCTION HISTORY

### Discovery History

Subsurface maps generated from coal borings indicated a Pennsylvanian bedrock structural high that was subsequently drilled for oil exploration in 1936. The discovery well, the Bartelso Oil and Gas No. 1 Trame (N1/2 SE NW, Sec. 8, T1N-R3W), established production of 115 barrels of oil per day (BOPD) from sandstones within the Mississippian Cypress Formation at a depth of 1,027 feet. In 1939, the Mosebach No. 1 Robben (SE SW SE, Sec. 5, T1N-R3W) was drilled to a total depth of 2,431 feet and established production of 162 BOPD from Silurian carbonates at 2,413 feet. Subsequent drilling eventually verified that the Silurian reservoir was a pinnacle reef.

### Production History

Since its discovery, Bartelso Field has produced approximately 4.7 million barrels of oil (MMBO) from a total of 530 productive acres. The Cypress pay was developed on 10-acre well spacing during primary production; the spacing for Silurian wells was set at 20 acres. Seventy-six wells have produced from the Cypress sands and 43 are currently productive. An additional 39 wells have been drilled for Silurian production.

Secondary oil recovery operations in the Cypress began in the early 1950s with the introduction of three waterfloods involving 24 injection wells and infill drilling of 27 production wells. The field has produced approximately 2.6 MMBO and 4.0 million barrels of water (MMBW) since waterflood operations commenced.



It is impossible to determine exact production amounts from the individual reservoirs because production numbers have been commingled. According to the operators, the Cypress portion of the total production amounts to approximately 2.5 MMBO.

## **RESERVOIR AND TRAP CHARACTERISTICS**

The Cypress Formation is approximately 100 feet thick at Bartelso and comprises fine-grained to very fine-grained sandstones interbedded with dark brown to light greenish gray shales. Individual Cypress sandstones in the field may be up to 60 feet thick, although thinner beds about 10 feet thick are more commonly hydrocarbon reservoirs. The Silurian reef facies, more than 900 feet thick here, are also productive. Discussions of Silurian reef reservoirs can be found in other Illinois State Geological Survey publications (e. g., Whitaker 1988).

### **Reservoir Geometry**

A structure map on the Beech Creek (Barlow) Limestone at Bartelso reveals two small structural domes with approximately 75 feet of closure (fig. 3). These structures are due to differential compaction around the Silurian pinnacle reef and the resultant draping of younger strata over the reef (Bristol 1974, Whitaker 1988). Production is concentrated on the crests and northern flanks of the structures, with the bulk of the Cypress production situated on the western of the two domes. The influence of these structures during Cypress time will be addressed in a later section on paleostructure.

The Cypress Formation was divided into four individual sandstone intervals, each separated by thin shale layers, using detailed stratigraphic correlations based on available wireline logs obtained within the field. These four sandstone intervals were labeled, in ascending order, pink, purple, gray, and red (fig. 4). The upper three of these sandstone intervals produce hydrocarbons at Bartelso, although the youngest (red) sand is the major reservoir. Preliminary regional mapping suggests that each of the thin shale layers separating the intervals correlates with regional shale beds. These regional shale beds apparently represent minor transgressive pulses.

Cross sections 1 to 4 (fig. 5) show the relationships between the four major sandstone intervals within the Cypress at Bartelso. The lowest interval (pink) displays a characteristically blocky signature on the spontaneous potential (SP) resistivity logs run in the field and is a relatively clean sandstone package. This interval is approximately 40 to 50 feet thick and contains numerous discontinuous shale beds. The distribution of the sandstone(s) within the pink interval is impossible to accurately determine because of the lack of penetrations into this sandstone, and thus the lack of cores and wireline logs. Semiregional mapping indicates the sandstones from this interval underlie the entire field area. No production has been recorded from this interval in this field.

The second sand interval (purple) is generally 10 to 15 feet thick and relatively continuous throughout the field (fig. 6). Interpretations of wireline logs indicate that shales are rare in this interval and that distinct compartments, if present, are difficult to document because of the lack of adequate control (fig. 5). Relative homogeneity of this sandstone interval is indicated by a consistent oil-water contact at -550 feet (fig. 6).

The distribution pattern of the sandstones within the purple interval suggests a shoreface deposit that was influenced by tidal currents. This sandstone probably represents a slightly shallower environment than that represented by the pink interval and suggests continued progradation of the Cypress delta complex.

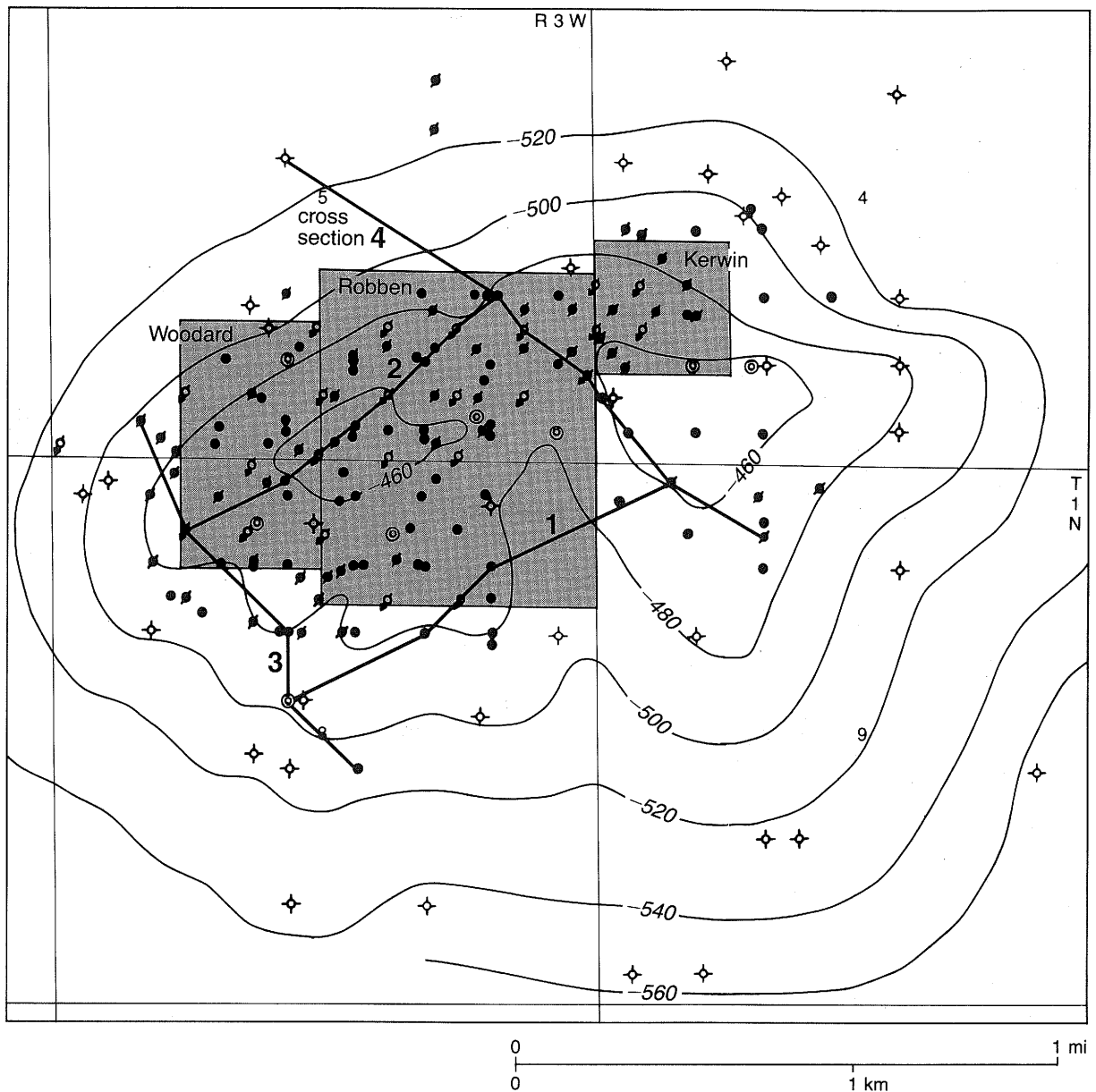


**Figure 3** Structure map on the top of the Beech Creek (Barlow) Formation at Bartelso Field (contour lines in feet). Location of cross section numbers 1, 2, 3, and 4 (fig. 5) are shown.

The third sand interval (gray) is dominated by siltstones and shales, although thin sandstone beds are present locally. On wireline logs, these sandstones display a suppressed SP deflection caused, in large part, by thin-bed resolution problems of the SP-resistivity tools used. The distribution of sandstone within the gray interval (fig. 7) suggests a small clastic influx into quiet water. Apparently, the sandstone is derived from a northwesterly source and may represent a very small delta formed by ebb tidal currents or a small crevasse splay. The original oil-water contact for this interval was at approximately -540 feet. Due to the reservoir geometry, this contact caused an isolated trap along the western, downdip flank of the field (fig. 7).

The youngest Cypress sandstone interval (red) comprises well-formed, discontinuous sand lenses that are locally multistoried (stacked). Relatively thick shales

Robert H. Robben  
 No. 1 Kohrman  
 T1N R3W  
 SW NE SE Sec. 5

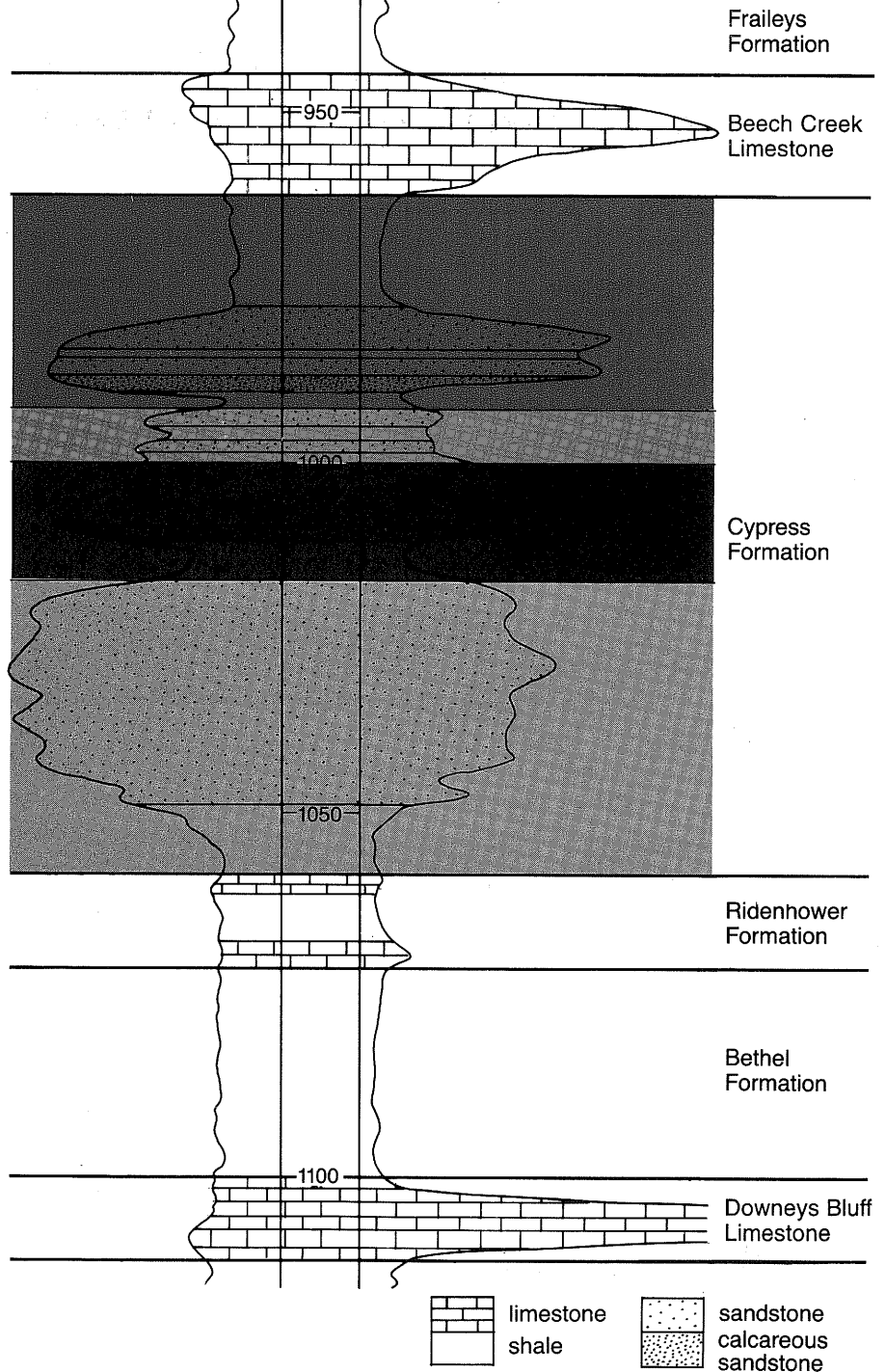


**Figure 4** Type log for the Cypress Formation at Bartelso Field. The log characteristics of the four sandstone intervals are illustrated.

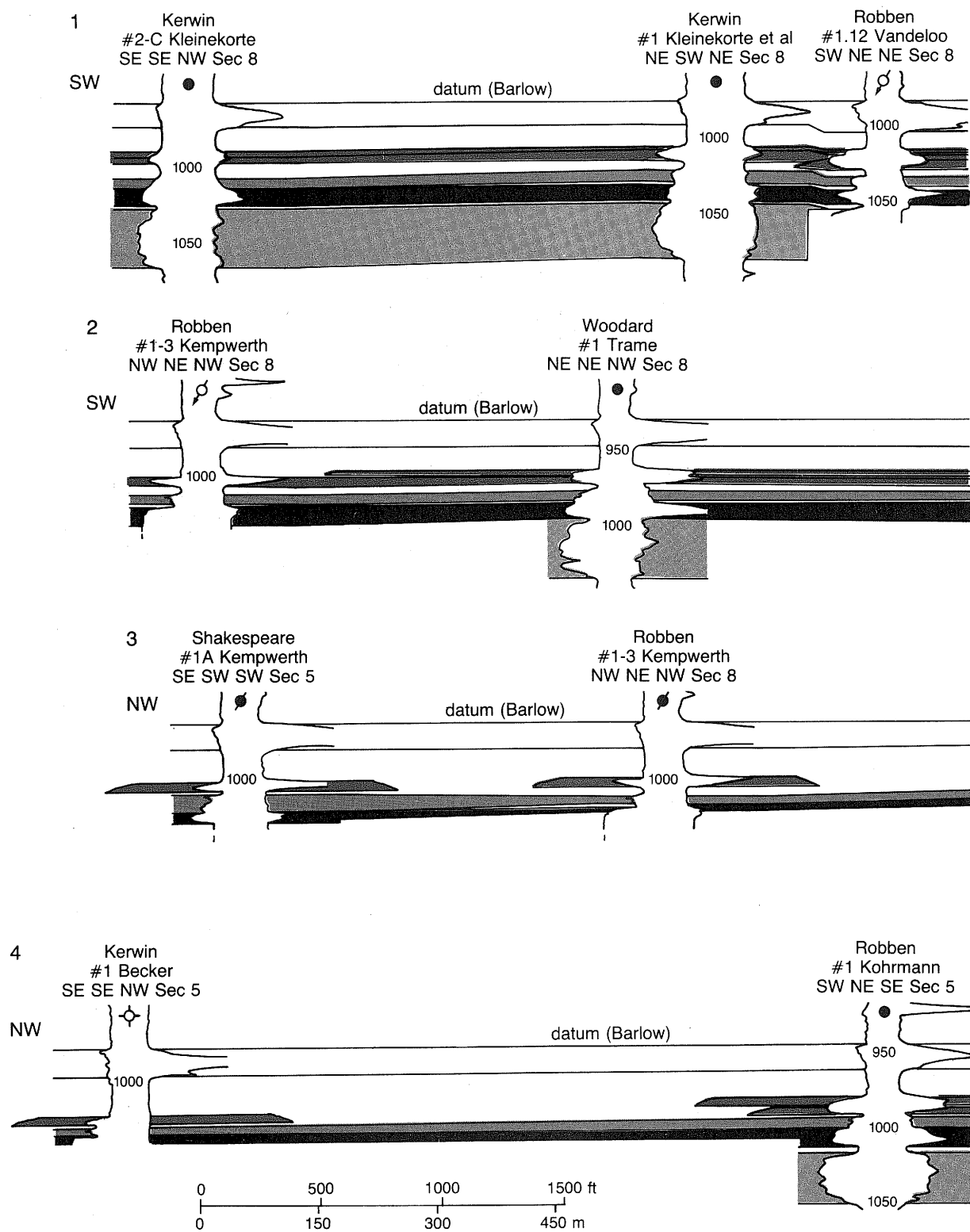
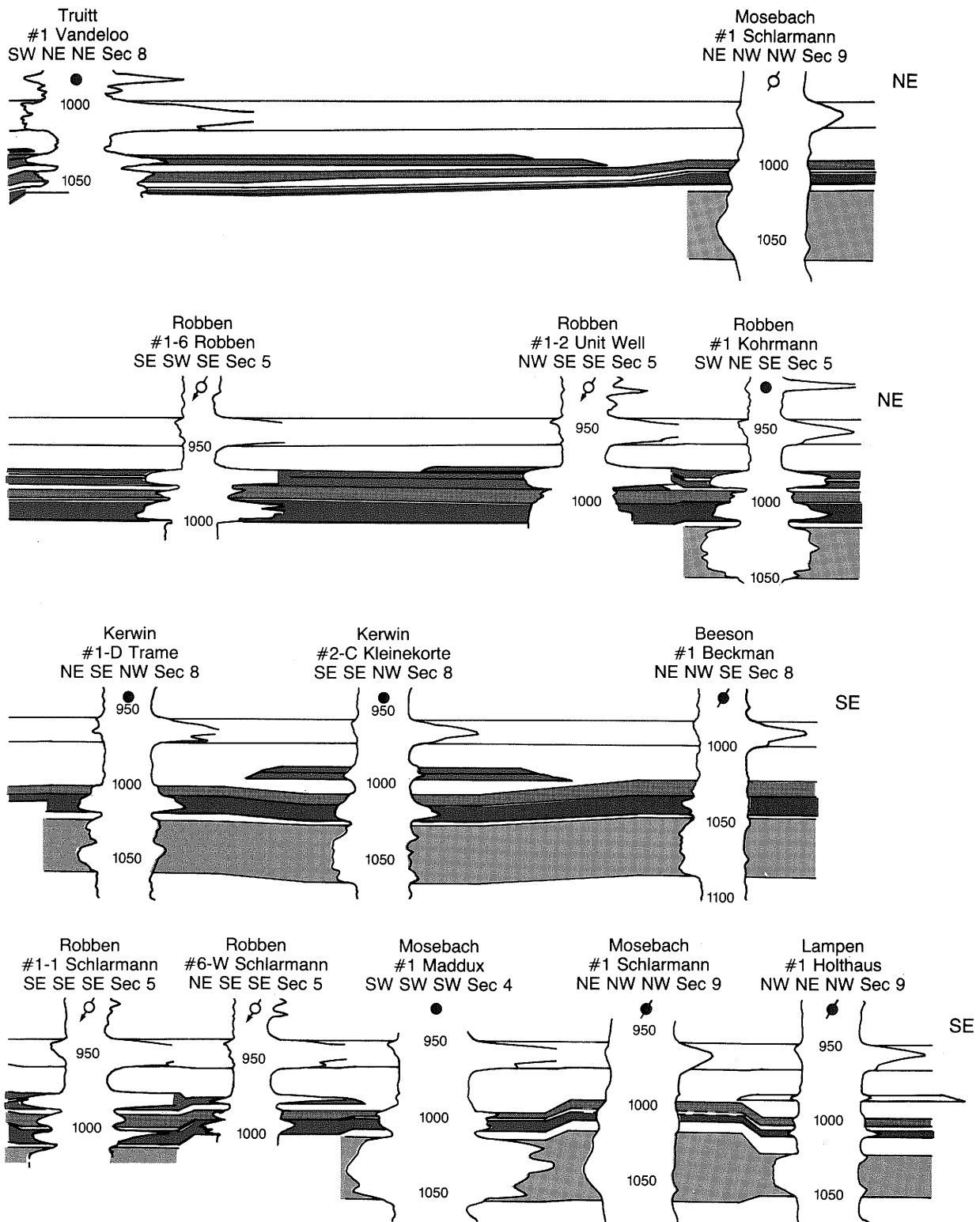


**Figure 5** Stratigraphic cross sections 1–4. Cross section 1 shows the variabilities in the sandstones within the four intervals; note the relative continuity of the sandstones within the red interval in a northeast–southwest direction. Cross section 2 shows three sandstones within the red interval, each separated by thin shales. A lack of suitable log suites makes the distribution of all three sandstones within the red interval impossible to map. Note the discontinuity of the sandstones within the gray interval.



Cross section 3 illustrates the discontinuity of the sandstones within the red interval in a northwest–southeast direction; note the differences in log character of the various sandstones within each interval. Cross section 4 shows the stacked nature of the isolated sandstones within the red interval in a northwest–southeast direction. Thin shale beds within the red interval apparently form barriers to fluid migration; however, the thin, discontinuous shale lenses within the purple interval do not substantially compartmentalize sandstones within that interval.

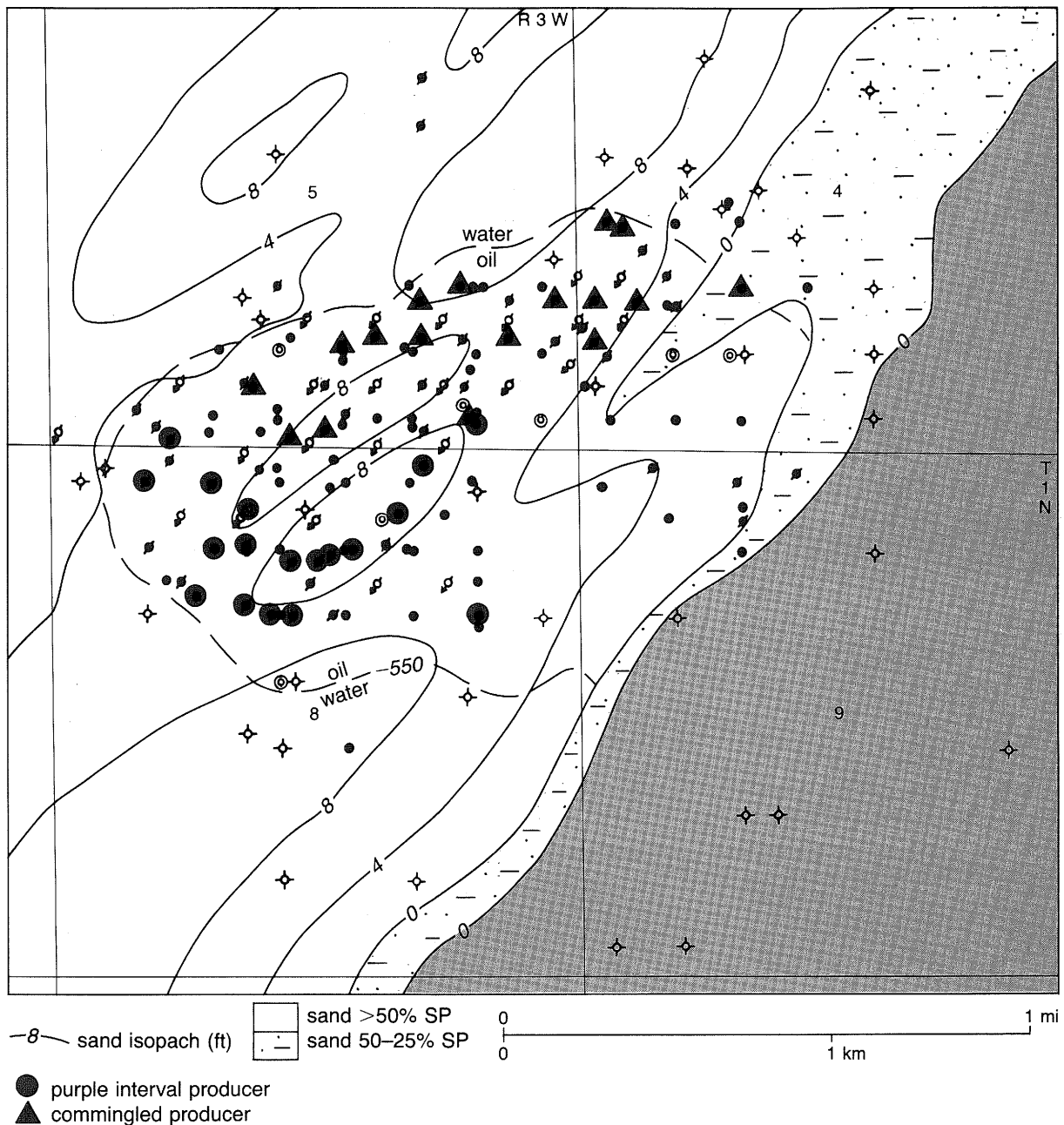


**Figure 6** Isopach map of clean sandstone within the purple interval. The geometry of this clean sandstone suggests an upper shoreface deposit. Note the single oil–water contact.

separate this interval from the underlying sands of the gray interval and the overlying Beech Creek (Barlow) Limestone. The northwest–southeast cross sections (1 and 2, fig. 5) illustrate that the red interval is characterized by distinct and separate sand bodies. These cross sections also suggest that the sandstone lenses may have been deposited in subtle paleolows. The northeast–southwest sections (3 and 4, fig. 5) show that the sands are more continuous in that direction.

Because data are more abundant in the red interval, sandstone distribution is more easily defined in it than in the other intervals. Detailed stratigraphic correlations enabled differentiation of several individual sandstone lenses within this interval,

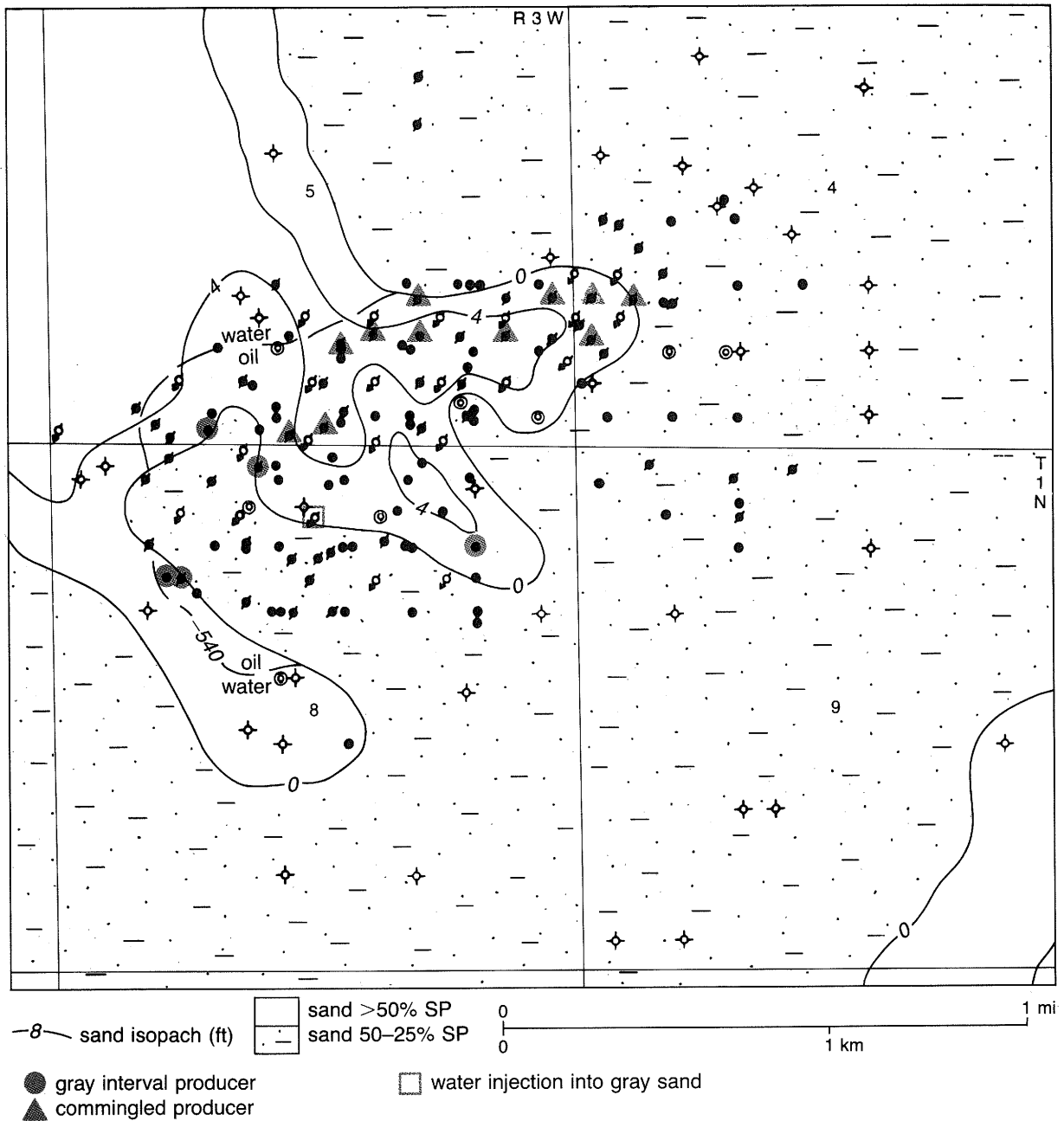


**Figure 7** Isopach map of clean sandstone within the gray interval. The geometry of the thin sandstone suggests a crevasse splay or some other higher energy influx of clastics deposited in quiet water. Note the isolated trap on the southwestern part of the structure and the presence of one oil–water contact.

each separated by thin shale layers (fig. 8a, b). The isolated nature and distinct orientation of these sandstones in a northeast–southwest direction suggest that they are marine bars. Two hypotheses for the origin of these bars are that they are offshore bar complexes oriented shore-parallel, or they are shore-normal tidal shoals. We favor the second hypothesis, which was originally suggested for some Chesterian sandstones by several workers (Potter 1962, 1963, Baker 1980, Williams et al. 1982, Specht 1985, Treworgy 1988), and will discuss it in more detail in a later section.

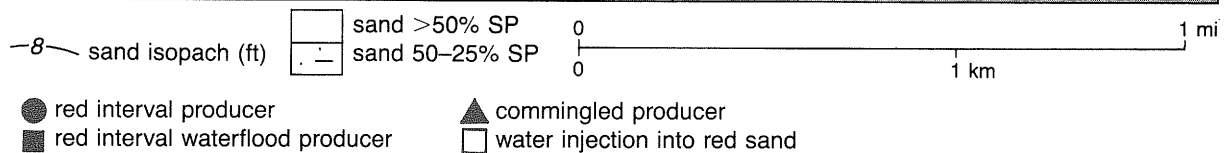
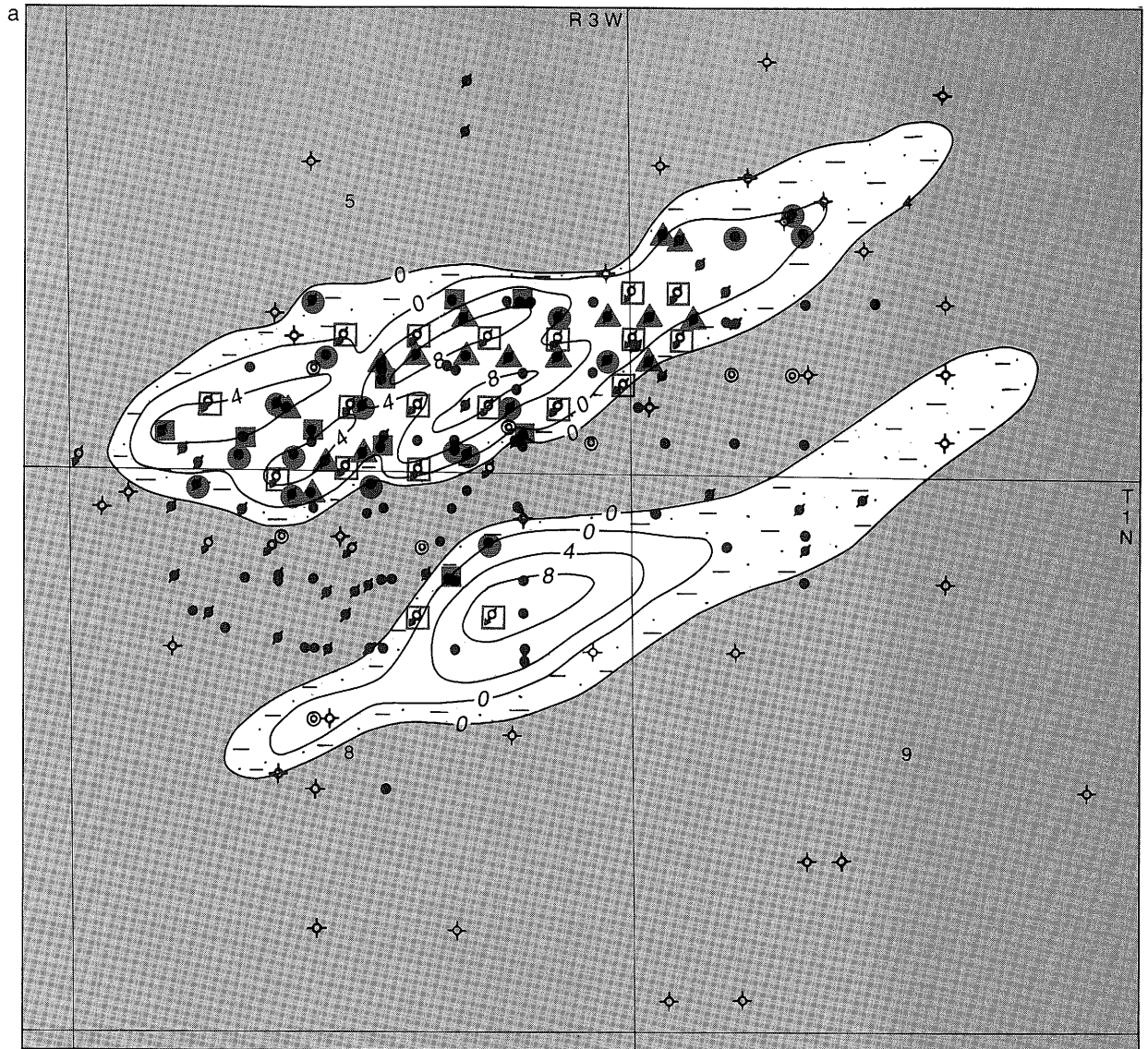
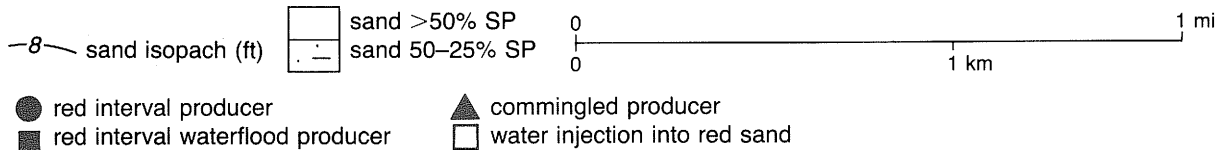
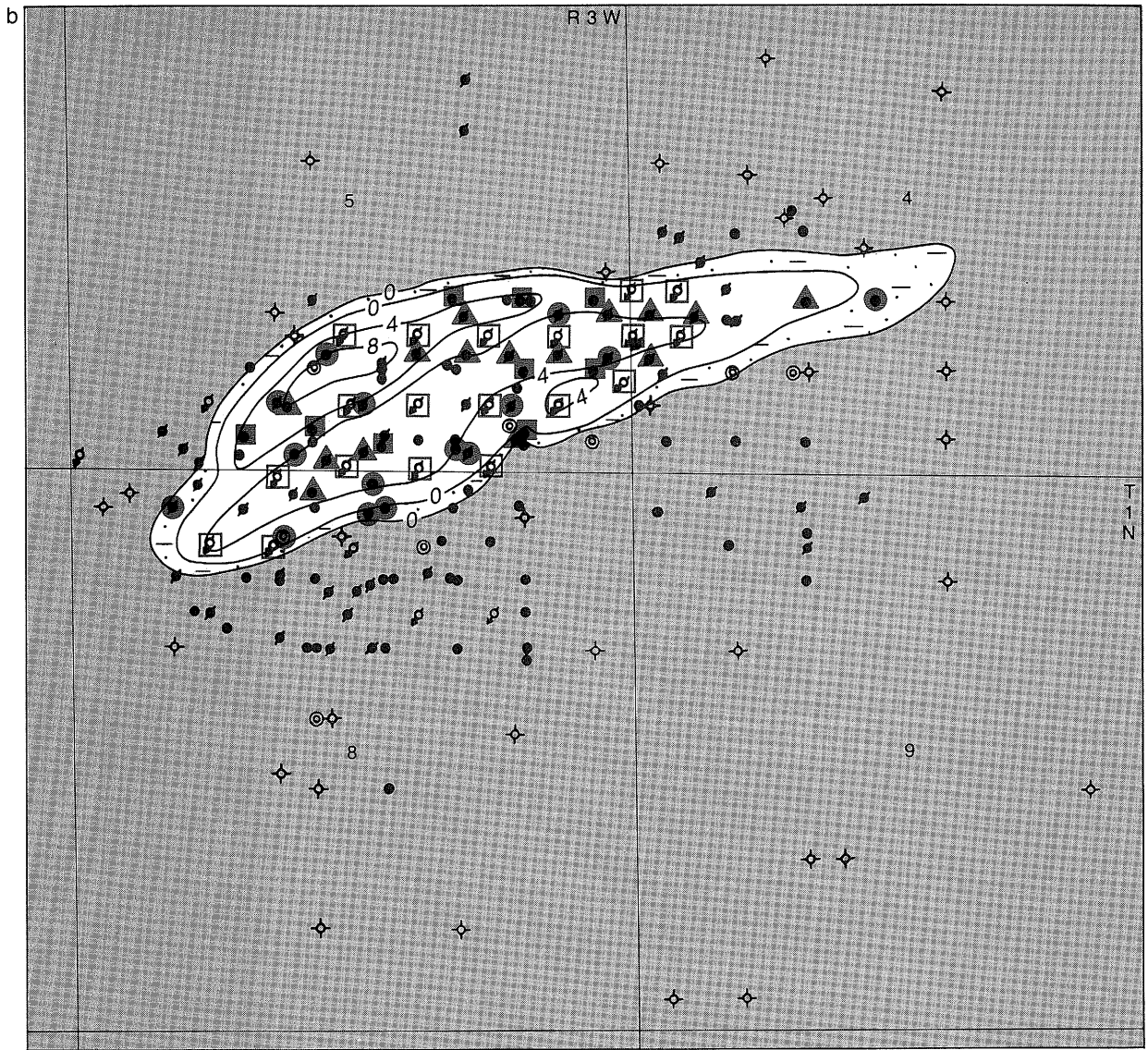


**Figure 8** Isopach maps of clean sandstone within the red interval. The geometry of the sandstones suggests that these bodies were deposited as offshore bars elongated in a northeast–southwest direction. The northern bar shown

The northern bar complex comprises at least two separate, stacked bars that are separated by a thin shale layer (cross section 4, fig. 5). This thin shale acts as an effective seal, as exhibited by drill-stem tests that indicated gas in the lower red sandstone; whereas, the upper red sandstone in the same wells tested only oil. These gas–oil relationships can best be explained if the updip, gas-saturated edge of a lower bar underlies an oil-saturated part of an upper bar. In fact, the sandstone thicknesses shown on the isopach maps in figure 8 suggest that the bar trends could be further subdivided into several smaller, shingled sand lenses. Unfortunately, further subdivision is difficult because of the poor resolution that is characteristic of the types of logs run in the field and of the lack of cores from the interval.





in (a) is overlain by the bar shown in (b), with a 6-inch to 2-foot-thick shale bed separating the two. This shale is effective enough as a seal to have enabled a modest gas cap to develop in the underlying bar.

### Paleostructural Influence

The absence of wireline logs from a substantial portion of the deeper wells makes determinations of paleostructure dubious. The structure at Bartleso is caused by draping over a reef. This draping is a result of differential compaction of Silurian sediments through time (Whitaker 1988). Because this differential compaction occurs slowly, periods of relatively constant deposition easily compensate for any slight topographic variations caused by this phenomenon. The topographic relief over the buried reef was probably never sufficient to have significantly affected deposition. Consequently, the distribution of the Cypress sands here was not likely the result of structural factors, but was instead the result of proximity to a source of

clastics, transport of sediment, and reworking of the deposits by marine currents. These factors will be discussed in the section on depositional environment.

### **Trap Type**

The trap type at Bartelso Field varies from structural to stratigraphic, depending on the Cypress interval involved. The continuous nature of communicative sands within the pink and purple intervals indicates that entrapment of hydrocarbons in these intervals would require a positive structural position. It is more difficult to determine whether the sands communicate within the gray interval, but the distribution and thin-bedded nature of these sands suggest that stratigraphy is at least as important as structure. This is particularly the case for the small, isolated accumulation along the western flank of the field (fig. 7). Hydrocarbon entrapment within the red interval is dependent, however, on stratigraphic rather than structural factors. The cleanliness of the sandstones and their position within a bar are of primary importance regarding reservoir development, oil-water ratios, and producibility.

### **Reservoir Lithofacies**

Evidence such as drilling cuttings, two cores from the field area, and cores from other fields suggests that the various sandstones within the Cypress Formation are remarkably similar in their lithologic characteristics. The sandstones are generally clean, moderately to fairly well-sorted, fine-grained to very fine-grained quartz arenites to subarkoses. Cementation is primarily due to silica, and lesser amounts of calcite and minor amounts of clay minerals, feldspar, and limonite.

The few core analyses run by operators in the study area have shown that clean Cypress sandstones have generally uniform porosity values that range from 16% to 22%. Permeabilities, however, vary in these same sands from less than 100 to more than 700 millidarcies. Two examples of the variability in porosity and permeability in core analyses are illustrated in figure 9.

Microscopic examinations of four thin sections from core samples from the red interval in the Mosebach No. 1 H. Kempwerth (SE SE SW SW, Sec. 5, T1N-R3W) revealed that the sandstone mineralogy is more than 90% quartz with minor amounts of feldspar, clay minerals, muscovite, chert, calcite, and very minor amounts of fossil fragments. Quartz grains exhibited abundant overgrowths, are thus subangular to angular in shape, and often occur in an interlocking mosaic. The absence of clay-mineral rims on the host grains made it difficult to identify their original outlines (pl. 1).

Feldspar grains, which constitute approximately 4% to 6% of the sandstones, are fine to very fine in size, and their shape varies from subrounded to angular, depending on the amount of postdepositional alteration. Dissolution has affected many of the feldspar grains, particularly some potassium feldspars and the more calcium-rich plagioclases. This dissolution has enhanced porosity to some degree and has also resulted in the development of microporosity (plates 2, 3). Albite overgrowths have been observed, but they are extremely rare.

Calcite cement was not abundant in any of the samples we examined from the No. 1 Kempwerth. When present, calcite is associated with widely dispersed fossil fragments and also appears as syntaxial overgrowths on echinoderm fragments (pl. 4).

Analysis of clay minerals revealed that the No. 1 Kempwerth contains minor amounts of kaolinite, chlorite, and illite (table 1). The clay mineral content in the samples was less than 2%. Most of the kaolinite is concentrated along a few thin bedding planes within the sandstone and may be partly detrital. Authigenic clay minerals are most plentiful near degraded muscovite grains and partially dissolved

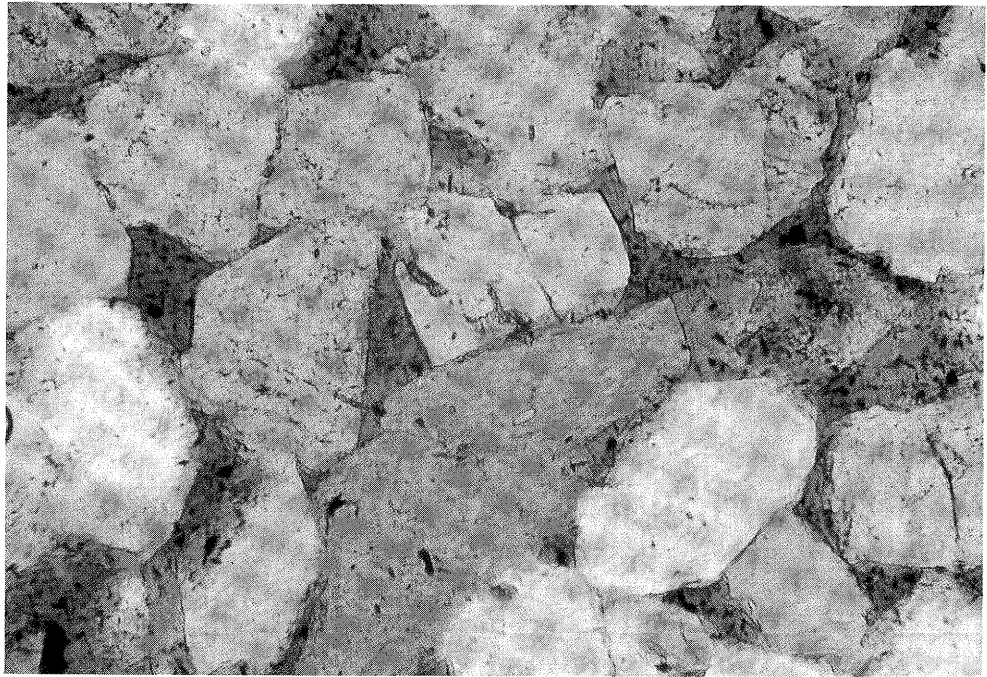


**Plate 1** Thin section from sandstone within the red interval (depth 1,000 ft) in the No. 1 Kempwerth reveals abundant quartz overgrowths that have partially occluded porosity.

125  $\mu\text{m}$

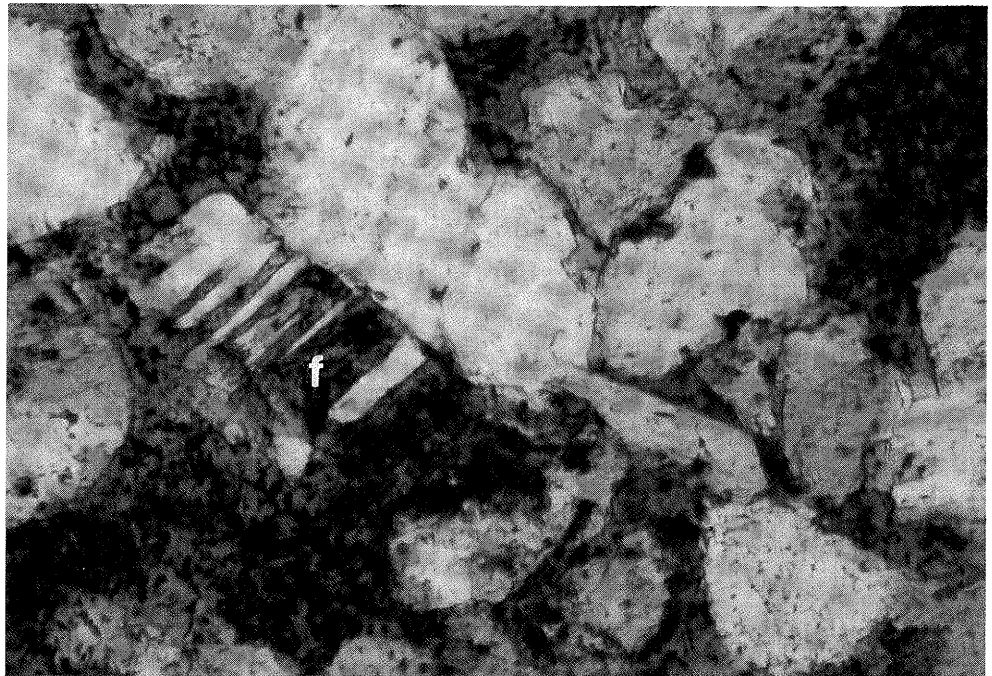


**Plate 2** Thin section from sandstone within the red interval (depth 1,003 ft) in the No. 1 Kempwerth showing partial dissolution of a feldspar grain (f).

125  $\mu\text{m}$

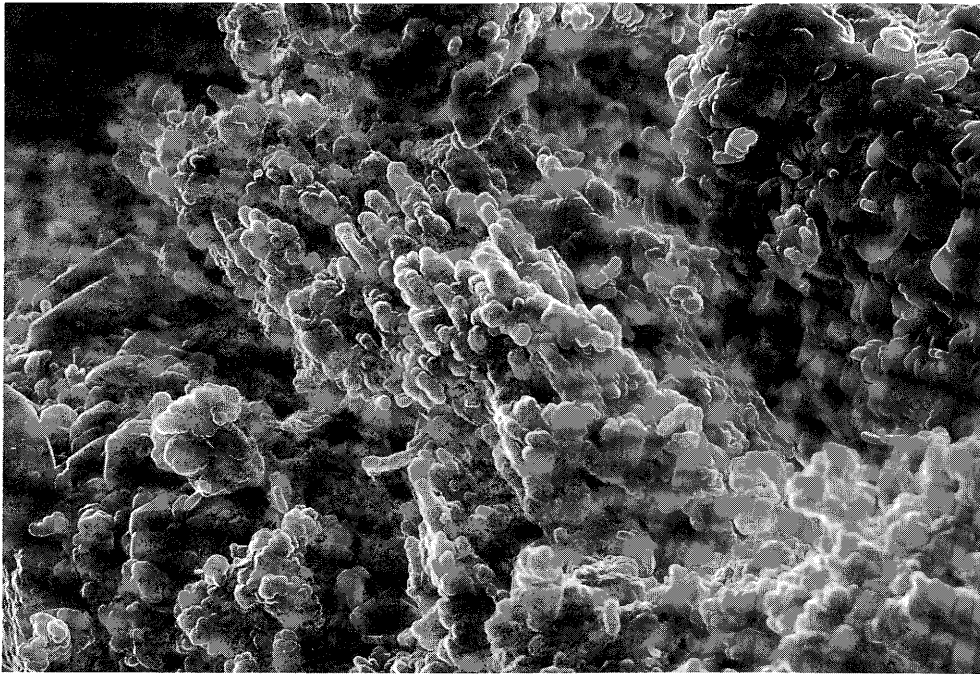


**Plate 3** SEM photomicrograph of a partially dissolved feldspar grain from the red interval (depth 1,006 ft) in the No. 1 Kempwerth.

20  $\mu$ m

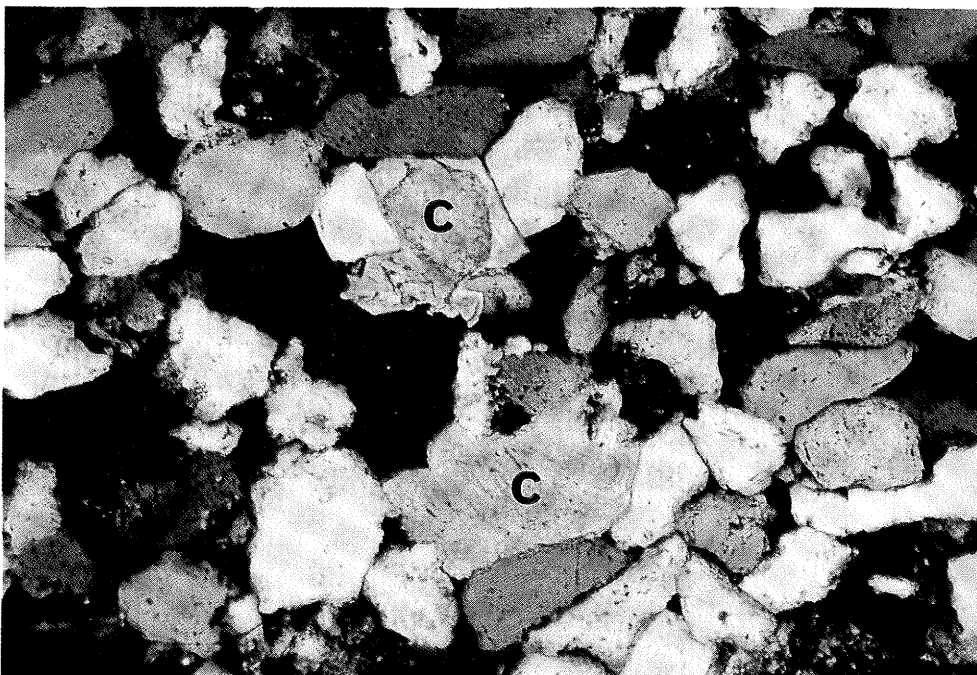


**Plate 4** Photomicrograph (under crossed nicols) of syntaxial calcite cement (c) on echinoderm fragment from the red interval (depth 1,000 ft) in the No. 1 Kempwerth.

250  $\mu$ m

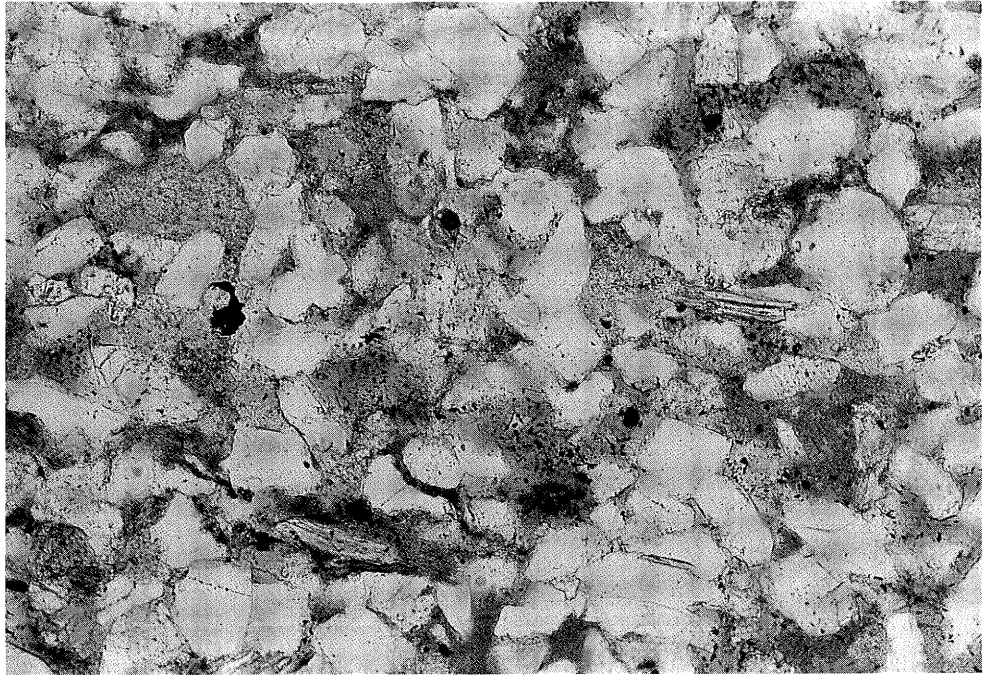


**Plate 5** Photomicrograph of clay minerals interspersed with sand grains from the red interval (depth 1,003 ft) in the No. 1 Kempwerth.

250  $\mu$ m

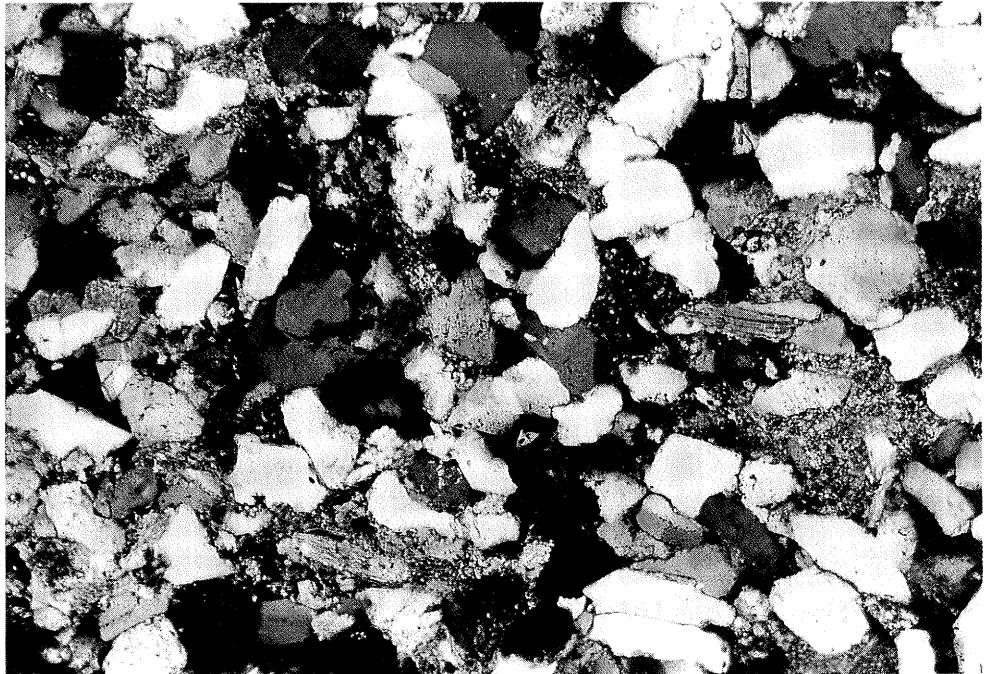


**Plate 6** Photomicrograph (under crossed nicols) of same section as plate 5.

250  $\mu$ m

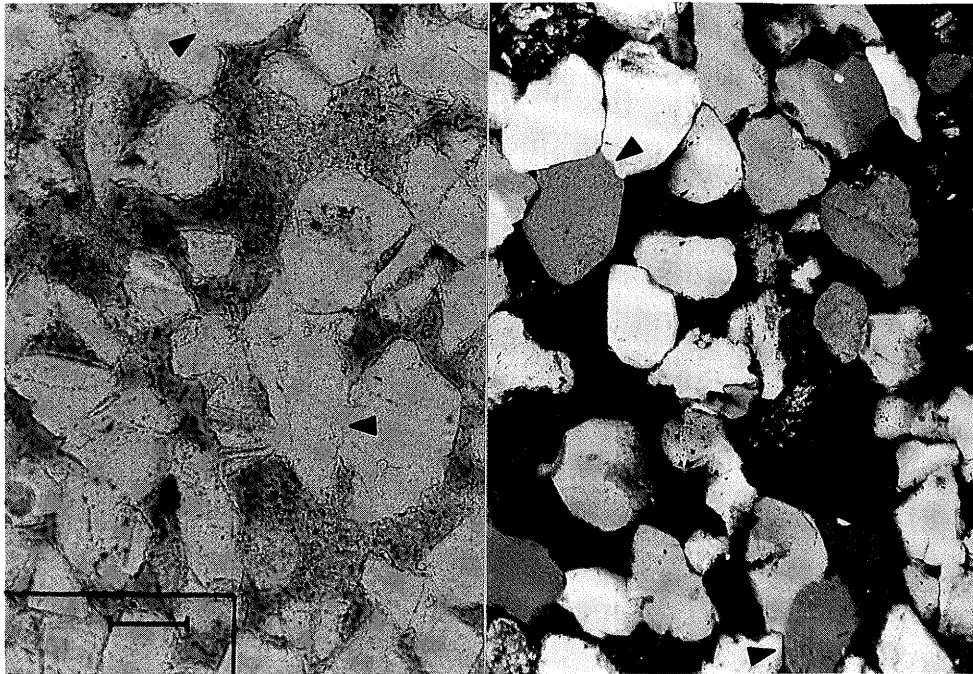


**Plate 7** Photomicrograph of quartz sand grains (depth 1,060 ft) from the No. 1 Hempen (right half under crossed nicols). Arrows indicate areas of possible pressure dissolution of sand grains.

250  $\mu\text{m}$

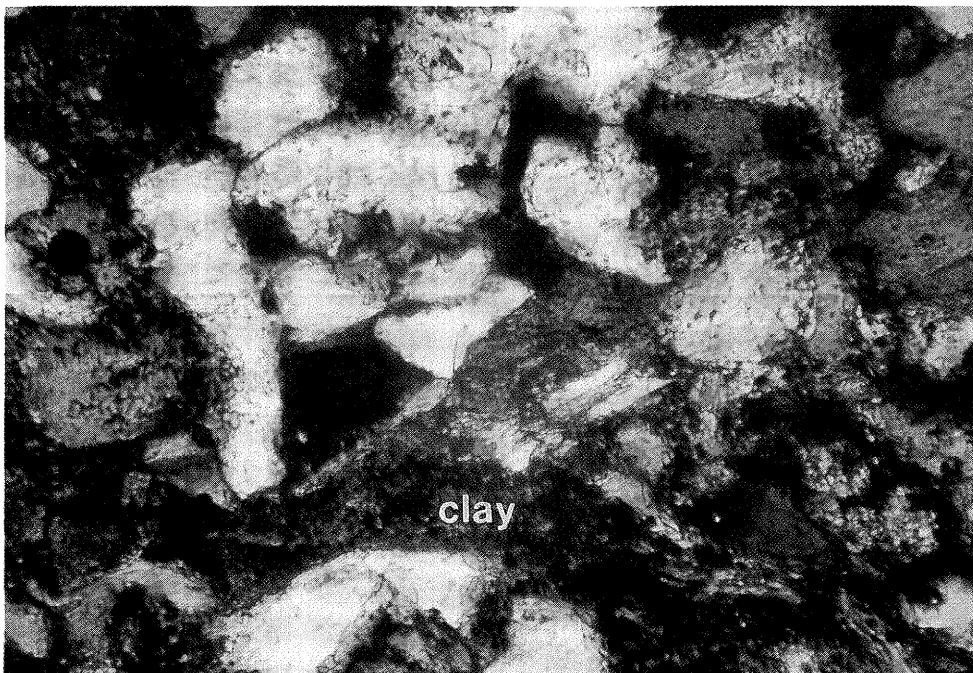


**Plate 8** Photomicrograph (under crossed nicols) of clay-mineral concentrations along a bedding plane within sandstone from the red interval (depth 1,003 ft) in the No. 1 Kempwerth.

125  $\mu\text{m}$

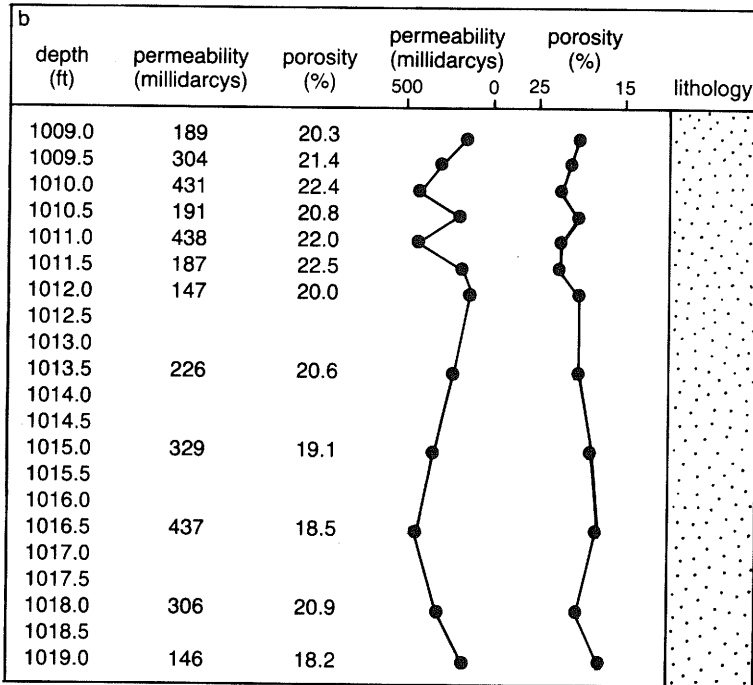
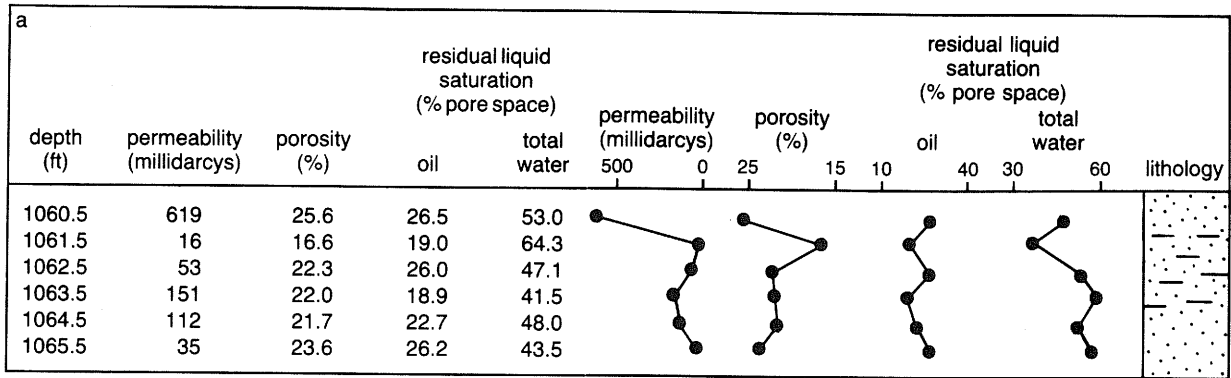


**Figure 9** Core analyses of (a) the red interval in the Ohio Co. No. 2 well (SE NE NW, Sec. 8, T1N-R3W) and (b) the purple interval from the Woofter No. 1 Hempen well (SE SW NE, Sec. 10, T2N-R3W). No logs were available from either well.

feldspars; the minerals can also be found scattered intermittently throughout the samples, and coat some sand grains (plates 5, 6). Quartz grains coated with an iron-rich chlorite that is interlayered with small amounts (5% to 15%) of a serpentine-like mineral generally exhibit less overgrowths than noncoated grains. Moore and Hughes (1991) are currently testing the hypothesis that chlorite-serpentine clay mineral coatings are a significant factor in porosity preservation (Heald 1965, Pittman and Lumsden 1968, Thomson 1982).

Core plugs taken from the purple-interval sandstone in the J. E. Woofter No. 1 Hempen (SE SE NE, Sec. 10, T2N-R3W), 5 miles north of Bartelso Field, revealed texture and mineralogy that are similar to red-interval sands at Bartelso. The sandstone appears moderately well sorted, porous, and moderately well cemented. Additionally, the sandstone exhibits low-angle crossbedding and thin clay laminae.

Only four thin sections could be made from the No. 1 Hempen plugs for microscopic examinations. As was the case in the No. 1 Kempwerth, the samples from the No. 1 Hempen exhibited abundant overgrowths that have modified the shapes of quartz grains to angular or subangular. Feldspar grains are generally subrounded to subangular, depending on the amounts of dissolution and albite overgrowths. Thin layers within the sandstone contain clay and possess correspondingly lower porosity. Authigenic clay minerals and calcite cement have only partially infilled

**Table 1** Mineral analysis of the clay-size particles from sandstone within the red interval in the No. 1 Kempwerth and the purple interval in the No. 1 Hemen.

depth (ft)	mineral analysis (%)								
	illite	illite/smectite	kaolinite	chlorite	quartz	K feldspar	plagioclase	calcite	dolomite
red interval, No. 1 Kempwerth									
- 1,060.5	0.5	0.2	2.9	0.1	94	1.3	0.7	0.5	0.0
- 1,061.5	2.2	1.3	4.4	1.6	73	11.1	5.6	0.1	0.5
- 1,062.5	1.3	0.8	3.8	0.9	83	0.1	9.7	0.2	0.3
- 1,065.5	0.7	0.6	1.2	2.9	87	1.9	5.4	0.2	0.1
purple interval, No. 1 Hemen									
- 997.0	0.3	0.0	1.5	0.2	70	0.5	27.3	0.2	0.0
- 1,000.0	1.3	0.4	3.0	0.6	89	1.0	3.3	1.2	0.0
- 1,003.0	2.1	1.2	5.3	1.4	87	0.8	1.3	1.0	0.2
- 1,006.0	1.3	0.8	2.9	0.6	89	1.5	0.7	2.8	0.1

pores. There are no wireline logs from this well, making it impossible to correlate SP or resistivity responses to the lithologic variations observed in the samples.

Analysis of clay minerals from the No. 1 Hemen (table 1) revealed that the clay-mineral content is slightly less than in the samples from the red interval in the No. 1 Kempwerth. Most of this decrease appears to be due to a lesser content of kaolinite within the thin clay-rich layers of sandstone.

In addition to the core samples from the area, numerous sample cuttings were examined from the entire Cypress interval. Because of the potential for caving in shallower strata, sample cuttings are not as reliable as cores for lithologic determinations. Nevertheless, we made several generalizations on the basis of the samples. All sandstones within the Cypress contain fragments of marine fauna. These fragments include echinoderms, ostracods, brachiopods, and trilobites. Siltstone, gray to green shale, and rare samples of coal were observed in the gray interval. We believe these coal samples to be in place because no other samples of coal were found from any other Cypress interval in the Bartelso area. Contamination from coal cavings would probably not have been limited to the few samples from the gray interval.

### Depositional Environment

The various intervals of the Cypress at Bartelso display evidence of different environments of deposition. In general, it appears that the Cypress was deposited during a prograding sequence that was eventually inundated during, or shortly after, deposition of the gray interval. The authors propose that this transgression was caused by a eustatic sea-level rise during a minor interglacial period. Stratigraphic evidence suggests that numerous relative fluctuations in the sea level that occurred throughout Chesterian time at a more rapid frequency than could be easily explained by tectonism. These fluctuations affected sedimentation throughout the region during the Carboniferous (Frakes and Crowell 1969, Robinson 1973, Rowley et al. 1985). Correlations with strata of similar age from other basins will be required to prove our assertion.

The Ridenhower Formation, which consists of thin limestones and intercalated limestones and shales, directly underlies the Cypress and represents what is called



a maximum flooding surface in the sequence stratigraphy nomenclature (Mitchum 1977, Van Wagoner et al. 1990). The pink interval, then, represents the initial progradational phase of the Cypress at Bartelso (the lower part of the highstand systems tract). Sandstones within this interval apparently were deposited across the shallow Illinois Embayment in a delta-front setting. Today, these sandstones comprise a relatively thick, continuous sequence that may be 40 to 50 feet thick in the Bartelso area. Small shale drapes can be observed in the few wireline logs that have been run in this interval throughout the field.

The shoreface sandstones within the purple interval are much thinner and apparently were affected by currents in a northeast-southwest direction, as indicated on the isopach map (fig. 6). The evidence indicates to us that these currents were probably tidal and may have been shore-normal (i.e., perpendicular to the advancing delta-induced shoreline).

The gray interval was a low-energy environment that was apparently affected by periods of minor clastic influx. The abundance of gray to green shales and rare coal fragments in this interval suggests that the main environment of deposition was shallower still than the underlying purple interval. This interval may represent a lowstand caused by a relative sea-level fall and would then mark the beginning of another sequence. The depositional setting is interpreted to be either tidal flat or coastal plain or possibly a combination of the two. The source for the clastics within this interval apparently was from the northwest (fig. 7) and may represent small crevasse splays.

Sandstones within the red interval were probably deposited as tidal shoals or bars located seaward of the underlying gray interval and oriented shore-normal. This interval represents the beginning of retrogradational deposits in the transgressive systems tract. The bars in the Bartelso area exhibit a shingled nature that can be seen on the cross sections (fig. 5) and isopach maps (fig. 8a, b). Currents tended to winnow out most of the clay-sized particles, leaving behind relatively clean, porous sandstones that were separated by thin shale layers. Continued transgression covered the sands of the red interval with shales, which are in turn overlain by the Beech Creek (Barlow) Limestone. The shales directly overlying the Beech Creek Limestone may represent another maximum flooding surface. A summary of our proposed sequence stratigraphy is provided in figure 10.

### **Diagenesis**

Postdepositional alterations of the Cypress sediments are in evidence from the rock samples. The diagenetic sequence for the Cypress at Bartelso Field (fig. 11) was interpreted on the basis of macroscopic and microscopic examinations of available well cuttings, eight thin sections, samples from two cores, and XRD analyses. One of the earliest diagenetic alterations occurred when small echinoderm fragments incorporated within the sands developed syntaxial overgrowths (pl. 6) almost immediately after burial (R. D. Cole, personal communication, 1990).

Continued compaction of the sands caused pressure dissolution of quartz grains, particularly polycrystalline quartz (pl. 7). This dissolution yielded silica-rich waters throughout the formation and enabled overgrowths to form on most of the quartz grains that partially occluded porosity (pl. 1). There were no apparent clay-mineral rims on the original sand grains, making it difficult to determine their original outline.

In addition to the relatively rare, scattered patches of early-stage calcite cement, wireline log signatures and well cuttings from several wells indicate the presence of a presumably later-stage calcite cement that is restricted to the lowest foot or two of sandstones in both the purple and red intervals (fig. 4). This cement was probably

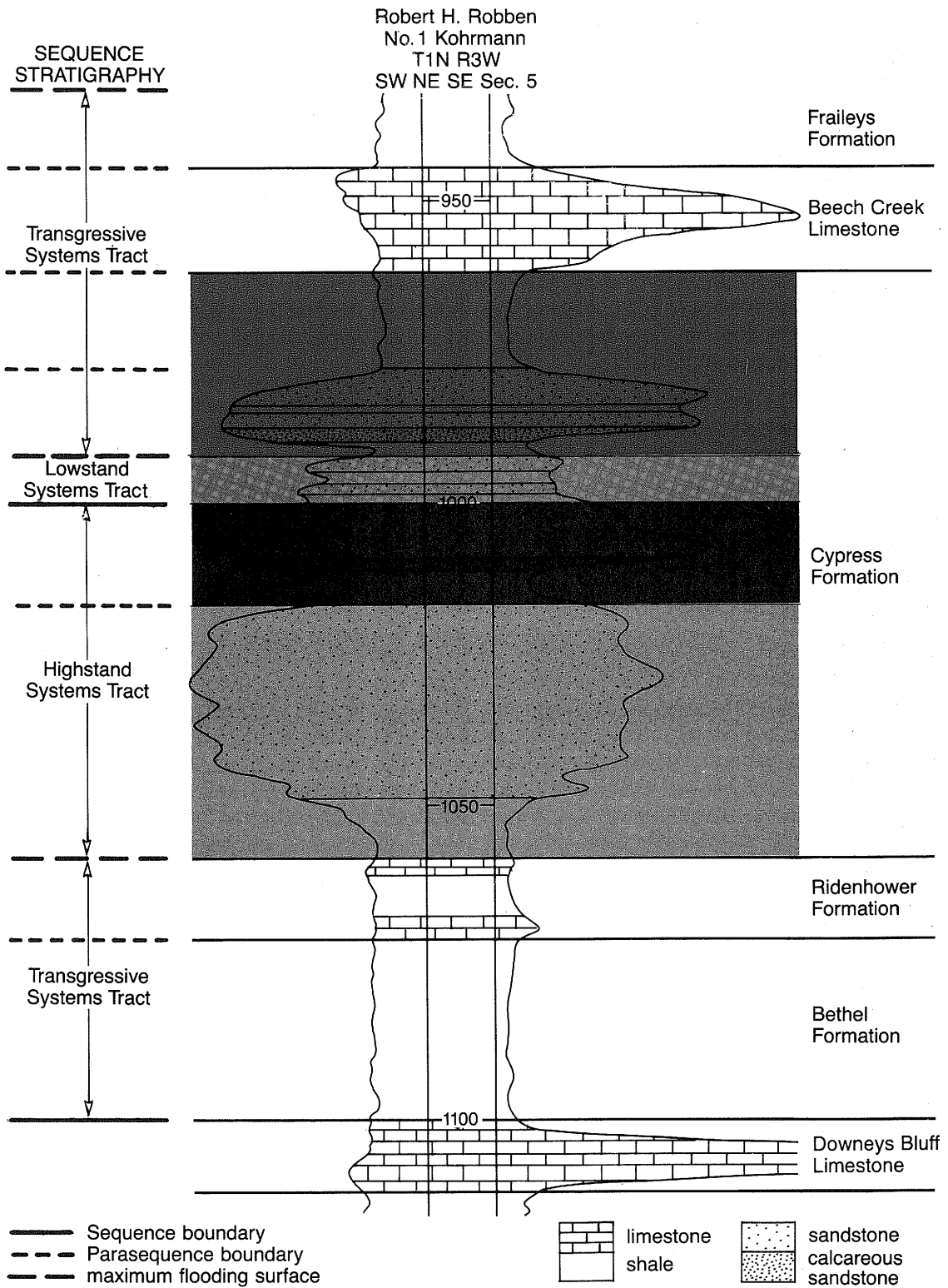


**Figure 10** Proposed sequence stratigraphy of the Cypress and adjacent intervals at Bartelso, as determined from preliminary regional studies of the lower Chesterian Series in southern Illinois.

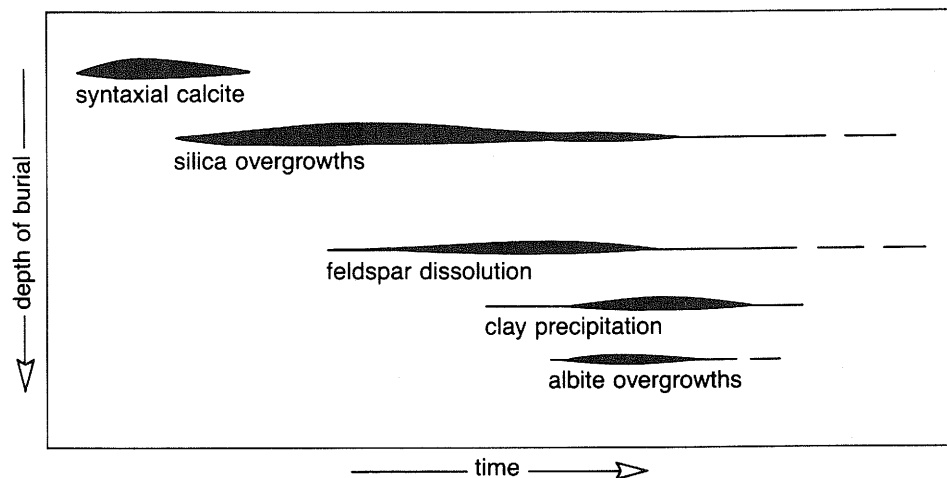


**Figure 11** Interpreted diagenetic sequence in the Cypress sandstones at Bartelso Field.

formed as dewatering of subjacent calcareous shales forced carbonate ions up into the basal parts of the overlying sandstones. This cement is not in evidence in all wells and was not observed in the thin sections.

The dissolution of some feldspar grains has, to some degree, enhanced porosity (plates 2, 3). Calcium-bearing plagioclases were probably subjected to the greatest degree of dissolution because they are generally unstable at normal reservoir pressures and chemistries. Potassium feldspars also show varying degrees of dissolution in the samples. The dissolution of feldspars has been discussed in numerous publications (e. g., Siebert et al. 1984, Dutton 1977) and is commonly thought to have been caused by slightly acidic brines formed during the early stages of organic maturation and dewatering in shales. Other factors within the brine chemistry may also cause instability in feldspars and promote their dissolution, but it is not our purpose to go into any great detail on these mechanisms. Whichever mechanism or combination of mechanisms was responsible for feldspar dissolution, it is believed that framework grain dissolution occurs at a moderate to deep burial depth and would therefore tend to happen well after initial diagenetic processes had commenced (Siebert et al. 1984). If aluminum ions are not flushed out of the sandstone, one of the possible byproducts of feldspar dissolution is precipitation of authigenic clay minerals. An additional byproduct of this dissolution is free silica, which could generate quartz overgrowths.

Authigenic albite formed as overgrowths on some feldspar grains and partially occluded porosity to a very minor degree. The more sodium-rich plagioclase grains (albite, oligoclase, and diagenetically albitized plagioclases) commonly act as hosts for albite overgrowth (Helmond and van de Kamp 1984), and the occurrence here apparently is no exception. Although oligoclase and albite hosts appear unaltered, albitized plagioclase hosts are mottled gray in plane light because of impurities in the original grain. Both kinds of grains are optically continuous with overgrowths.

Authigenic chlorite, illite, and mixed-layer illite/smectite are scattered on many of the quartz overgrowths and appear to be slightly more abundant in the areas near detrital clay-mineral concentrations (pl. 8). These authigenic clay minerals do not rim the original grain outlines, suggesting that the clay minerals precipitated after the onset of quartz overgrowths. There do not appear to be sufficient quantities of the authigenic clay minerals to cause major reductions in porosity, although permeability is probably affected to some degree. As mentioned earlier, the precipitation of layered chlorite-serpentine clay minerals may have actually preserved

porosity by coating many of the early- to middle-stage quartz overgrowths and preventing further overgrowths (Heald 1965, Pittman and Lumsden 1968, Thomson 1982, Moore and Hughes 1991).

## **Summary**

The quality of reservoirs within the Cypress Formation at Bartelso is affected by depositional environment more than by any other single factor. A depositional model for the Cypress is presented in figure 12. The best reservoirs are generally from the clean sandstones found in the marine-bar environment of the red interval (fig. 12d). Compartmentalization is probably a factor in this reservoir. The shoreface sandstones of the purple interval (fig. 12b) are also good reservoirs, but trapping mechanisms may not exist because these sandstones are laterally continuous over relatively large areas. The thin, discontinuous sandstones deposited in the paralic environments of the gray interval (fig. 12c) are relatively poor reservoirs because of their limited extent and the probable clay content. Sandstones within the pink interval (fig. 12a) are not productive at Bartelso, and not enough field-data were available to ascertain their potential reservoir quality. Sample examinations indicate that these sandstones are also clean and should make good reservoirs if a trapping mechanism is present.

Diagenesis plays a role in affecting porosity and probably accounts for some of the variations seen in permeability. Whereas predictions of depositional environments can be made and thereby improve development and exploration strategies, not enough information is available to make predictions of diagenetic patterns. Authigenic clay minerals are present, but probably not in sufficient quantities to pose major production problems.

## **CLASSIFICATION AND IDENTIFICATION OF PLAYS**

Our findings, based on the study at Bartelso Field, suggest there are at least four plays (production zones) in the Cypress Formation. Each individual play may require different strategies for exploitation.

### **Delta Front**

Sandstones deposited in this play, represented by the pink interval, would be subject to depositional patterns and reservoir compartmentalization that are common to the environment of deposition (i.e., occasional clay drapes, moderate current direction indicators, potentially large sandstone deposits, possible communication over large areas depending on effectiveness of shale seals). Outcrop studies of the Cypress Formation in progress at the Illinois State Geological Survey (R. D. Cole, personal communication, 1990) and examinations of sample sets from this interval suggest that these delta-front sandstones were deposited in a shallow sea, but in the subtidal realm. This play requires an associated structural closure because there appears to be sufficient communication between individual sand lenses to preclude stratigraphic entrapment of hydrocarbons. The fact that this interval contained no commercial hydrocarbons at Bartelso, despite the presence of a structure, suggests that the shale layer overlying the pink sands was not an adequate seal. Correlations with wireline logs in the field verify this supposition. Even though this interval does not contain hydrocarbons at Bartelso, it is nevertheless a viable play, provided adequate seals and structures can be defined.

### **Upper Shoreface**

The second play, represented by the purple interval, is characterized by sediments deposited in shallow marine conditions along the upper shoreface slightly seaward

from the overlying gray interval. Reworking of the sands by what we interpret to be tidal currents has given a northeast–southwest orientation to this sandstone. Sandstones within this play are relatively thin, contain a moderately small amount of clay, and may be laterally continuous over their area of deposition. In general, an associated structure would be necessary for hydrocarbon entrapment because of the continuity of the sandstones. The thin nature of these deposits may provide some opportunities for stratigraphic pinchouts.

### **Coastal Plain**

A third play, represented by the gray interval, involves sandstones deposited within low-energy environments associated with proximity to a shoreline. These environments include coastal plains, tidal flats, and possibly lagoons to estuaries. The thin and discontinuous sandstones within this play could be the result of tidal reworking, small tidal channels, or possibly small crevasse splay deposits. The geometry of these sandstones will be variable, depending on the particular geologic process responsible for their creation. Hydrocarbon traps within this play could be numerous and would not require structural closure, but reserves are probably limited because of the discontinuous nature of the sands. In general, this play would not be economical except as a secondary reservoir.

### **Marine Bars**

The fourth Cypress play is illustrated by the sandstones within the red interval. These sandstones may be very clean in the bar core and are generally deposited as elongate, isolated lenses oriented in a northeast–southwest direction. The sandstone bodies are commonly stacked and/or shingled, and separated by thin clay layers that may preclude communication between sandstones. The strong northeast–southwest orientation of the sands should make exploration and development of the sands relatively straightforward. Hydrocarbon entrapment within this play would be mainly stratigraphic and not require the presence of structural closure.

The source of these sandstones was either an offshore bar, which would result in bars oriented shore-parallel, or it was a tidal shoal/bar, which would lead to bars forming seaward of distributary mouths oriented shore-normal. We believe that the latter interpretation should be pursued as an exploration model.

The offshore bar hypothesis implies that the paleoshoreline, being parallel to the bars, was oriented northeast to southwest. This paleoshoreline may have been local, formed along the northeast–southwest flank of an individual deltaic lobe. Another possibility is that deltaic activity within this part of the basin had shifted sufficiently away from the area to cease to influence shoreline configuration. The bars would have shifted northward to northwestward as the shoreline retreated during transgression.

The tidal shoal (tidal bar) hypothesis implies that the bars were deposited parallel to, and seaward of, distributary channels as the deltaic system continued to be drowned by the advancing Cypress sea. Modern analogues indicate that macrotidal ranges coupled with low wave energy and low littoral drift are necessary for the development of tidal bars (Duane et al. 1972, Swift et al. 1973, Swift 1975). Little has been done, however, to examine this requirement in extremely shallow intracratonic settings. The paleoslope within the embayment that became the Illinois Basin is estimated to have been less than one tenth of 1° during Chesterian time. It is possible that because of these dips, less dramatic tidal ranges may have produced features similar to those seen today along coastal shelf areas under macrotidal and mesotidal conditions. The tidal bars would have advanced northeastward as the delta was inundated by the transgressing sea. Minor shifts in the

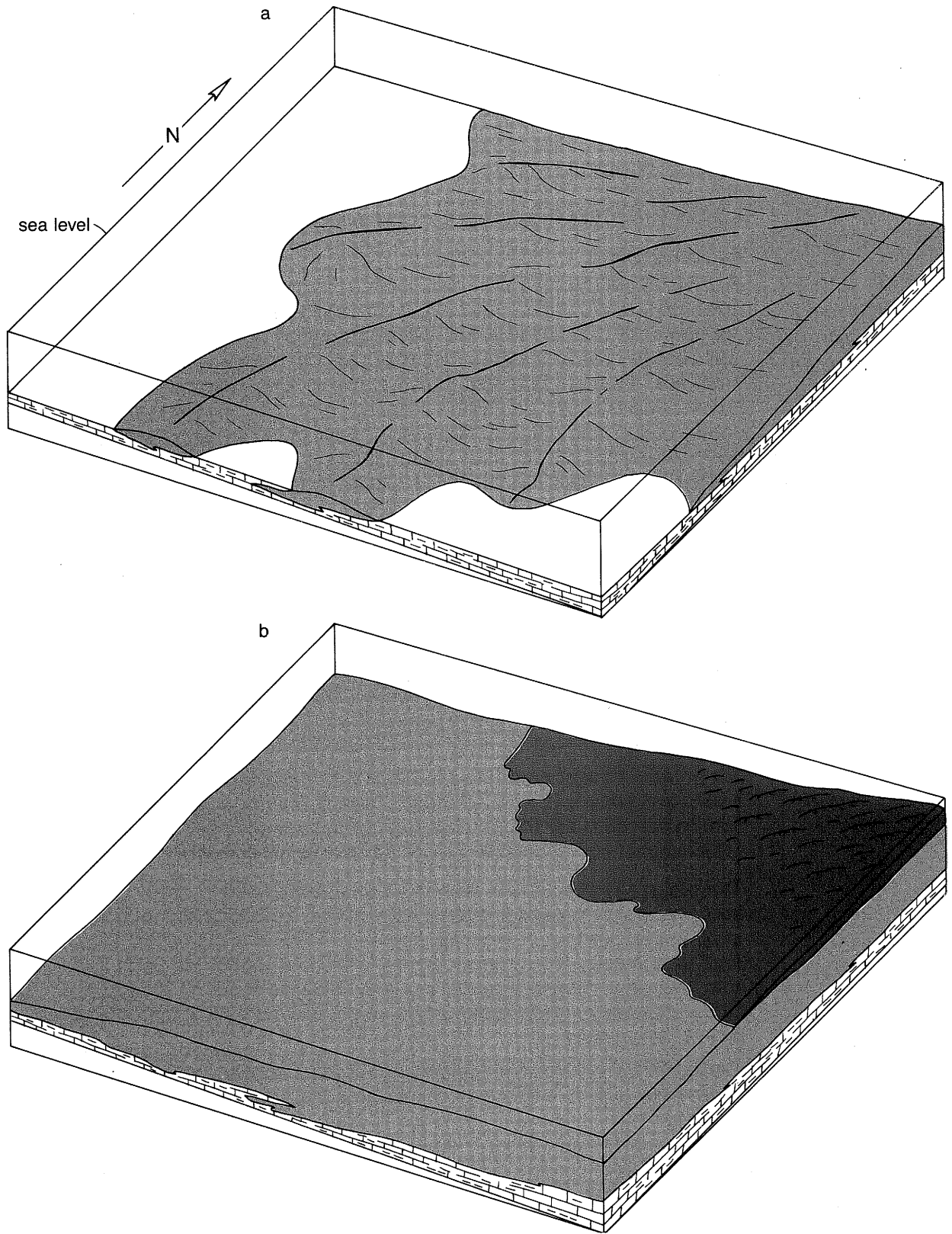
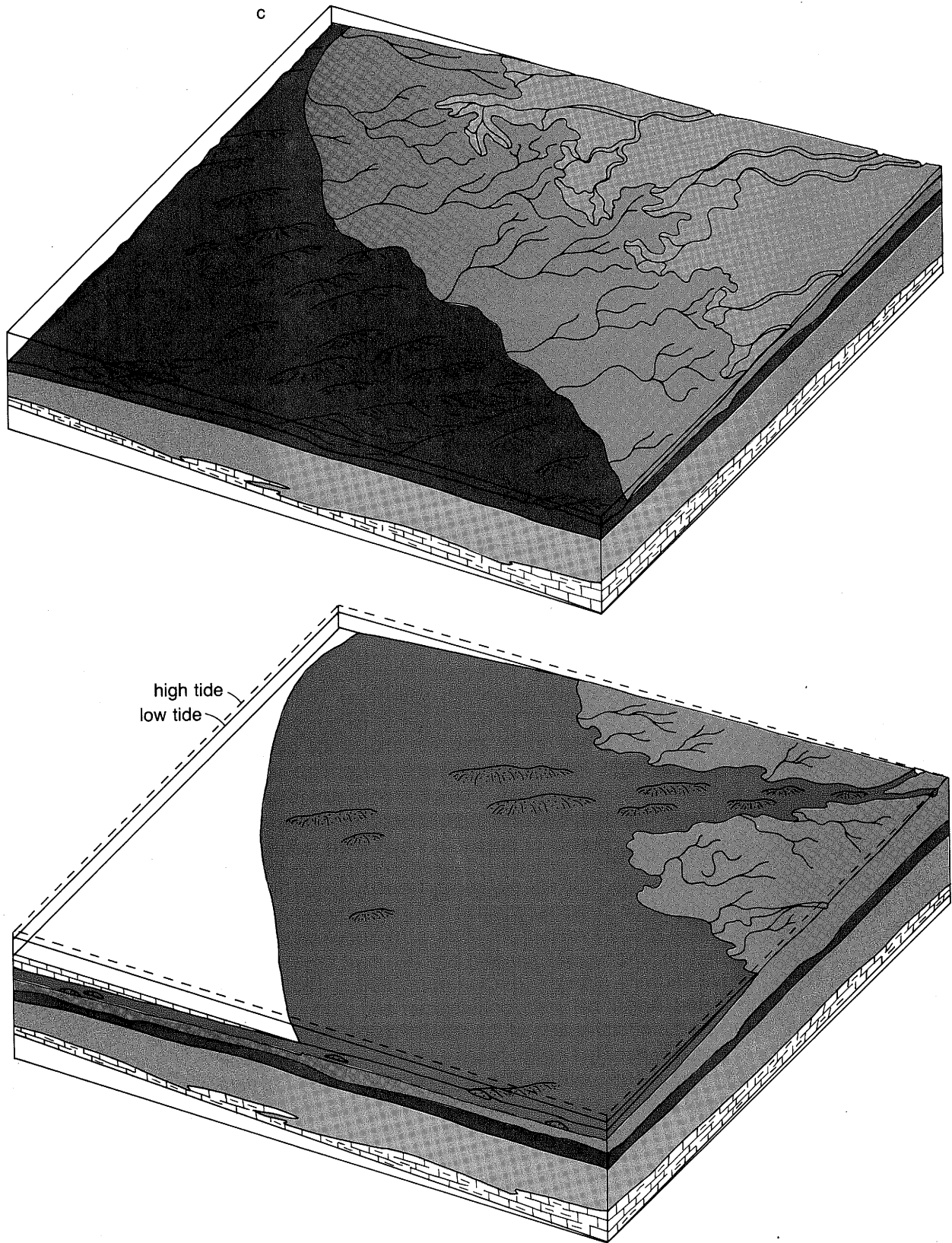


**Figure 12** Depositional model for the Cypress at Bartelso Field. (a) Delta front sands of the pink interval advance into the Bartelso area. (b) Minor transgressive pulse deposits a thin shale over the sands of the pink interval immediately prior to a renewed progradation that deposits sands of the purple interval in a continuing upward-shallowing sequence. Tidal influence oriented in a northeast-southwest direction is evident in these deposits. (c) An apparent relative sea level



fall enabled rapid progradation, resulting in tidal flat to delta plain environments of the gray interval. Shales and silts predominate although thin sands and infrequent coal deposits are also noted. (d) Transgression inundates the deltaic environments and results in the marine shales and offshore bars of the red interval. Clean sands are generally deposited as isolated shore-normal tidal bars oriented in an east–west to slightly northeast–southwest direction.

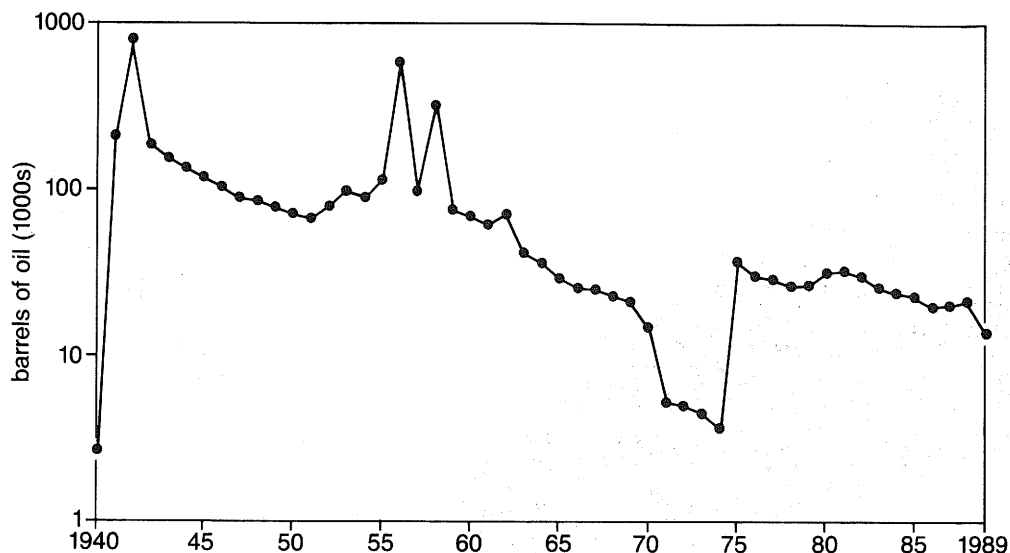


**Figure 13** Production decline curve for Bartelso Field (Cypress and Silurian reef reservoirs commingled).

## PRODUCTION CHARACTERISTICS

### Drilling and Completion Practices

The majority of wells in Bartelso Field have been drilled with rotary tools using fresh water-based muds, although some wells were drilled with cable tools. The Cypress sandstones were commonly fractured with 20 to 40 quarts of nitroglycerin and completed as open-hole producers. Wells drilled after the mid-1950s generally perforated through casing set through the pay zone. Little to no acidization was performed within the Cypress wells at the field. Pumping units are the main extraction tools for both primary and secondary recovery operations.

### Injection and Production Data

Cypress production was established in 1936 and peaked in the early 1940s (fig. 13). Enhanced recovery operations in the Cypress began in 1952 with the introduction of three waterfloods involving 24 injection wells on the crest of the Bartelso structure. The waterfloods were based on 10-acre well spacing and five-spot injection patterns. The production curve shows a standard decline from 1939 to 1952, when waterflooding was first initiated. Additional wells, both injector and producer, were drilled off-pattern to enhance the effectiveness of the flood. Production peaked in the mid-1950s and then gradually declined again, but at a slightly higher level than would be projected from the pre-1952 curve. This suggests that the flood was improving recovery rates within the Cypress. Many of the Cypress wells were temporarily shut-in during the early 1970s for pressure maintenance purposes, leading to a dramatic drop in production in those years. Cypress production resumed in 1975 under a coordinated fieldwide flood and a few more wells were drilled to enhance efficiency. Production decline rates from that period to the present were noticeably more gradual and suggest that the waterflood efficiency had increased

Injection of approximately 7.2 MMBW resulted in the production of about 1.25 MMBO and 5.25 MMBW from Cypress reservoirs. Injection water has consisted of a 50% mixture of produced Cypress and Bethel brines. No data or analyses have been published pertaining to the compatibility of this mixture with formation fluids in the Cypress.



**Table 2** Analyses of Cypress oil samples from Bartelso Field.

Year	API gravity	Sulfur content	Viscosity
1940	36.2°	0.2%	NA
1953	36.9°	0.2%	6.3 cp @71° F

The Kerwin waterflood (fig. 3) involved 40 acres with five injection and five production wells. The flood injected 1 MMBW and produced 132,100 BO and 186,500 BW between 1952 and 1963. The Robben waterflood (fig. 3) involved 200 acres with 14 injection and 19 production wells. The flood produced 619,200 BO and approximately 1 MMBW between 1953 and 1963. The Woodard waterflood (fig. 3) is currently operating and involves 80 acres with five injection and three production wells. The flood has injected 3.2 MMBW and produced 500,000 BO and 3.5 MMBW since 1954. Apparently, the injection pattern adequately waterflooded the sandstones from the red interval (fig. 8). This is not to suggest that this pattern would be effective in all cases because the geometry of the shingled sandstones may not be so well suited to such symmetrical spacing. Downdip parts of the purple and gray intervals were not sufficiently subjected to secondary recovery methods (figs. 6 and 7) and probably still contain some movable hydrocarbon reserves. The viability of extracting any remaining hydrocarbons from the purple or gray intervals depends on the operator's economics.

### **Oil Characteristics**

Carlton (1940) sampled oil from Bartelso and the Robben waterflood project reported oil characteristics before the flooding began in 1953. The results of these two analyses are summarized in table 2.

Analyses of three oil samples gathered in 1990 from Bartelso Field are shown in appendix A. Chromatograms of analyses from the saturated parts of these samples are presented in appendix B. These samples are all from reservoirs within the red interval that have been subjected to waterfloods. The sample characteristics are consistent with Illinois Basin samples that were sourced from the New Albany Shale (Upper Devonian). Sample EOR-69 contains more than 1% asphaltenes, significantly different from other samples in the field. Asphaltenes can cause some production problems, particularly when acidizing with HCL, when adding low surface tension fluids such as diesel fuel, and when using CO<sub>2</sub> injection for enhanced oil recovery projects (Newberry and Barker 1985).

### **Water Characteristics**

Seven samples of the formation brine from Cypress reservoirs at Bartelso are summarized in appendix A. Because of the mixtures of Bethel and Cypress brines for waterflooding, these samples do not indicate true Cypress brine characteristics. One interesting observation is the relatively low concentrations of chlorine in these brines.

### **Original Volumetrics**

Volumetrics were calculated for three of the Cypress reservoirs in Bartelso Field. We used the standard formula:

$$7758 \times \text{reservoir acre-feet} \times \text{porosity} \times (1 - \text{water saturation}).$$

We calculated the values of reservoir acre-feet from the isopach maps, assigned porosity by using average values obtained from core analyses in the area, and calculated water saturation from wireline logs. The results are as follows:

purple interval: shoreface  $7758 \times 2954 \times 0.20 \times 0.6 = 2,979,000$  BO  
 gray interval: coastal plain  $7758 \times 551 \times 0.20 \times 0.7 = 592,000$  BO  
 red "A" interval: marine bar  $7758 \times 588 \times 0.20 \times 0.8 = 729,000$  BO  
 red "B" interval-north: marine bar  $7758 \times 782 \times 0.20 \times 0.8 = 971,000$  BO  
 red "B" interval-south: marine bar  $7758 \times 443 \times 0.20 \times 0.8 = 550,000$  BO  
**Original oil in place = 5,821,000 BO**

The commonly used formation volume factor for Cypress reservoirs in the basin is 1.15 (B. Podolsky, personal communication, 1991). We therefore calculated the original stock tank barrels of oil in place for the Cypress to be 5.062 MMBO.

Estimated primary recovery from the Cypress at Bartelso, based on operator estimates, was 1.25 MMBO. Secondary recovery accounts for another 1.25 MMBO. The recovery factor for combined primary and secondary methods is therefore approximately 49%. This extraordinarily high recovery rate may be a result of an erroneously optimistic estimation of the Cypress portion of the total reserves produced, inaccurate assumptions on the volumetric calculations leading to erroneously low estimates of reserves, or the high efficiency of the primary and secondary recovery methods used. We believe that the recovery efficiency figures are relatively accurate and, if anything, are slightly conservative. The combination of the coordinated flood and other recovery methods used in the field were more effective than is commonly the case in the Illinois Basin.

## DEVELOPMENT AND PRODUCTION STRATEGY

The lack of existing cores from the field precludes obtaining engineering data on flow measurements or flow modeling. Therefore, we limit our discussion on development and production strategy to conclusions and observations made on the existing data.

The production practices used at Bartelso Field lead to an overall recovery efficiency for the Cypress of more than 49%. Assuming that the calculations are relatively accurate, these observations indicate that a 10-acre well spacing and a five-spot waterflood program with infill drilling were adequate to effectively drain the Cypress red interval at Bartelso. The recovery rate probably would have been higher had the sandstones within the purple and gray intervals been waterflooded adequately.

### Recommendations

A standard 10-acre well spacing apparently is not adequate to efficiently drain all of the sandstones within the Cypress Formation, if they are distributed as at Bartelso Field. In the red interval, the bar complexes exhibited reservoir shingling (fig. 8a, b), indicating the potential benefits of closer spacing in this environment. Off-pattern producers drilled for the waterflood project almost certainly encountered compartments that would otherwise not have been effectively drained. In addition, the western limit of the reservoir within the gray interval at Bartelso (fig. 7) is of a peculiar geometry that may not lend itself to efficient drainage by a 10-acre well spacing. It is always important to recognize the Cypress reservoir type to plan an optimum recovery strategy.

Secondary recovery methods should likewise be influenced by the type of reservoir that is being exploited. Separate waterflood projects may be required for each reservoir. Sweep efficiencies will obviously be affected by the geometries and

internal architecture of the individual reservoir. As a result, uniformly spaced wells on a secondary recovery project would probably not efficiently drain multiple reservoir types. This was probably the case at Bartelso.

Although clays did not apparently pose a significant threat to production at Bartelso, attention must be paid to the presence of clays to ensure that excessive formation damage does not result from improper drilling or completion practices.

The best way to plan an effective production program is to obtain cores from each reservoir and have a thorough analysis performed to determine optimum methods. The lack of engineering data from Bartelso makes more specific recommendations impossible.

## **ACKNOWLEDGMENTS**

We thank numerous people at the of the Illinois State Geological Survey for their helpful guidance and assistance in the generation and review of this manuscript. R. D. Cole, J. P. Grube, and H. E. Leetaru provided geologic input for the manuscript. Sample preparations for petrographic analyses were done by D. S. Beaty. Examinations and photographs from the scanning electron microscope were provided by B. Seyler. Clay analyses were performed by R. E. Hughes and D. M. Moore. The collection and analyses of oils and brines were supervised by I. Demir and G. L. Salmon.

This report is part of a major research project for reservoir classification and improved and enhanced oil recovery, cofunded by the U. S. Department of Energy (Grant DE-FG22-89BC14250) and the Illinois Department of Energy and Natural Resources(Grant AE-45). Their funding and dedication to the goals of this research are gratefully acknowledged.

## REFERENCES

- Baker, R. J., 1980, Geology of the Big Clifty Formation in the Wheatonville Consolidated Oil Field in Gibson County, Indiana: M.S. thesis, Ball State University, Muncie, 85 p.
- Bristol, H. M., 1974, Silurian Pinnacle Reefs and Related Oil Production in Southern Illinois: Illinois State Geological Survey, Illinois Petroleum 102, 97 p.
- Carlton, J. L., 1940, The geology of the Bartelso Oil Field, Clinton County, Illinois: M. S. thesis, University of Chicago, 58 p.
- Duane, D. B., M. E. Field, E. P. Meisburger, D. J. P. Swift, and S. J. Williams, 1972, Linear shoals on the Atlantic inner shelf, Florida to Long Island, *in* D. J. P. Swift, D. B. Duane, and O. H. Pilkey, editors, Shelf Sediment Transport, Process and Pattern: Dowden, Hutchinson, and Ross, Stroudsburg, PA, p. 447-498.
- Dutton, S. P., 1977, Diagenesis and porosity distribution in deltaic sandstone, Strawn Series (Pennsylvanian), north-central Texas: Gulf Coast Association of Geological Societies Transactions, v. 27, p. 272-277.
- Frakes, L. A., and J. C. Crowell, 1969, Late Paleozoic glaciation: I. South America: Geological Society of America Bulletin, v. 80, p. 1007-1042.
- Heald, M. T., 1965, Lithification of Sandstones in West Virginia: West Virginia Geological and Economical Survey, Bulletin 30, 28 p.
- Helmond, K. P., and P. C. van de Kamp, 1984, Diagenetic mineralogy and controls on albitization and laumontite formation in Paleocene arkoses, Santa Ynez Mountains, California, *in* D. McDonald and R. Surdam, editors, Clastic Diagenesis: American Association of Petroleum Geologists, Memoir 37, p. 239-276.
- Mitchum, R. M., 1977, Seismic stratigraphy and global changes of sea level, part I: Glossary of terms used in seismic stratigraphy, *in* C. E. Payton, editor, Seismic Stratigraphy-Applications to Hydrocarbon Exploration: American Association of Petroleum Geologists Memoir 26, p. 205-212.
- Moore, D. M., and R. E. Hughes, 1991, Varieties of chlorites and illites and porosity in Mississippian sandstone reservoirs in the Illinois Basin: American Association of Petroleum Geologists, v. 75, no. 3, abstract and poster session, p. 639.
- Newberry, M. E., and K. M. Barker, 1985, Formation damage prevention through the control of paraffin and asphaltene deposition: Society of Petroleum Engineers Paper 13796, p. 53-58.
- Pittman, E. D., and D. N. Lumsden, 1968, Relationship between chlorite coatings on quartz grains and porosity, Spiro Sand, Oklahoma: Journal of Sedimentary Petrology, June, p. 668-670.
- Potter, P. E., 1963, Late Paleozoic Sandstones of the Illinois Basin: Illinois State Geological Survey, Report of Investigations 217, 92 p.
- Potter, P. E., 1962, Late Mississippian Sandstones of the Illinois Basin: Illinois State Geological Survey, Circular 340, 26 p.
- Robinson, P. L., 1973, Palaeoclimatology and continental drift, *in* D. H. Tarling and S. K. Runcorn, editors, Implications of Continental Drift to the Earth Sciences: Academic Press, London, p. 451-476.

- Rowley, D. B., A. Raymond, J. T. Parrish, A. L. Lottes, C. R. Scotese, and A. M. Ziegler, 1985, Carboniferous paleogeographic, phytographic, and paleoclimatic reconstructions: *International Journal of Coal Geology*, v. 5, p. 7–42.
- Siebert, R. M., G. K. Moncure, and R. W. Lahann, 1984, A theory of framework grain dissolution in sandstones, *in* D. McDonald and R. Surdam, editors, *Clastic Diagenesis: American Association of Petroleum Geologists, Memoir 37*, p. 163–175.
- Specht, T. H., 1985, Subsurface study of the Big Clifty Formation in southwestern Indiana: M.S. thesis, Indiana University, Bloomington, 48 p.
- Swift, D. J. B., 1975, Sand ridges and shoal retreat massifs: *Marine Geology*, v. 15, p. 227–247.
- Swift, D. J. B., D. B. Duane, and T. F. McKinney, 1973, Ridge and swale topography of the middle Atlantic bight, North America: Secular Response to the Holocene hydraulic regime: *Marine Geology*, v. 15, p. 227–247.
- Thomson, A. 1982, Preservation of porosity in the deep Woodbine/Tuscaloosa trend, Louisiana: *Journal of Petroleum Technology*, May, p. 1156–1162.
- Treworgy, J. D., 1988, The Illinois Basin — A Tidally and Tectonically Influenced Ramp during Mid-Chesterian Time: Illinois State Geological Survey, Circular 544, 20 p.
- Van Wagoner, J. C., R. M. Mitchum, K. M. Campion, and V. D. Rahmanian, 1990, Siliciclastic sequence stratigraphy in well logs, cores, and outcrops: American Association of Petroleum Geologists, *Methods in Exploration Series*, no. 7, 55 p.
- Whitaker, S. T., 1988, Silurian Pinnacle Reef Exploration in Illinois: Model for Hydrocarbon Exploration: Illinois State Geological Survey, Illinois Petroleum 130, 32 p.
- Williams, D. A., M. C. Noger, and P. J. Gooding, 1982, Investigation of Subsurface Tar-Sand Deposits in Western Kentucky; A Preliminary Study of the Big Clifty Sandstone Member of the Golconda Formation (Mississippian) in Butler County and Parts of Edmonson, Grayson, Logan, and Warren Counties: Kentucky Geological Survey, Information Circular 7, Series XI, 25 p.

## APPENDIX A RESERVOIR FLUID ANALYSIS

API Number 1202703143

Operator Newton

Well Name Gross No. 5

Location C SE SW, Sec. 5 ,T1N-R3W

Perforations Depth 987-997 ft (open hole) Cypress red interval

Surface Elevation 470 ft (Kelly bushing)

Waterflooded yes, presently inactive

### Brine Analysis

Brine sample number EOR-B17

Temperature (C) 25

Resistivity 0.166 ohm-m

Eh (mV) -279

pH 6.72

### Anion chemistry (mg/L)

Br	<1	I	<1
Cl	33980	NH <sub>4</sub>	179
CO <sub>3</sub>	<1	NO <sub>3</sub>	140
HCO <sub>3</sub>	416	SO <sub>4</sub>	44

### Cation chemistry (mg/L)

Al	1.26	Co	0.2	Mo	<0.08	Si	4.47
As	3.2	Cr	0.5	Na	17810	Sr	102
B	3.51	Cu	<0.06	Ni	<0.15	Ti	0.07
Ba	248	Fe	0.42	Pb	<0.4	V	0.27
Be	0.0007	K	65	Rb	<10	Zn	<0.02
Ca	856	Mg	556	Sb	0.5	Zr	0.04
Cd.	<0.05	Mn	0.15	Se	1.5		

### Oil Analysis

Oil sample number EOR 16

#### Hydrocarbon fraction (%)

saturated hydrocarbons	63.47
aromatic hydrocarbons	32.49
resins	3.71
asphaltenes	0.33

#### Selected hydrocarbon ratios

C17/C18	1.175
pristane/phytane	1.448
pristane/C17	1.240
phytane/C18	1.529

**APPENDIX A** *continued*

**API Number** 1202704175

**Operator** Kerwin

**Well Name** C.P. Maddux No. 9

**Location** SW NE SW, Sec. 4, T1N-R3W

**Perforations Depth** 991-996 ft Cypress red interval

**Surface Elevation** 460 ft (Kelly bushing)

**Waterflooded** yes

**Brine Analysis**

**Brine sample number** EOR-B19

**Temperature (C)** 25

**Resistivity** 0.136 ohm-m

**Eh (mV)** -111

**pH** 6.98

**Anion chemistry (mg/L)**

Br	<1	I	<1
Cl	35340	NH <sub>4</sub>	155
CO <sub>3</sub>	<1	NO <sub>3</sub>	118
HCO <sub>3</sub>	144	SO <sub>4</sub>	<1

**Cation chemistry (mg/L)**

Al	1.44	Co	<0.07	Mo	<0.08	Si	3.81
As	2.7	Cr	0.53	Na	18620	Sr	103
B	2.82	Cu	<0.06	Ni	<0.15	Ti	0.07
Ba	26.1	Fe	37.6	Pb	<0.4	V	0.33
Be	0.0028	K	66	Rb	<10	Zn	<0.02
Ca	1013	Mg	586	Sb	1.2	Zr	0.05
Cd	<0.05	Mn	1.07	Se	1.3		

**Oil Analysis**

**Oil sample number** EOR-17

**Hydrocarbon fraction (%)**

saturated hydrocarbons	69.99
aromatic hydrocarbons	24.77
resins	4.58
asphaltenes	0.66

**Selected hydrocarbon ratios**

C17/C18	1.209
pristane/phytane	1.358
pristane/C17	1.545
phytane/C18	1.736

**APPENDIX A** *continued*

**API Number** 1202701157

**Operator** Robben

**Well Name** Schlarmann No. 0,7

**Location** SW SE SE, Sec. 5, T1N-R3W

**Perforations Depth** 985-985.5 ft Cypress red interval

**Surface Elevation** not reported

**Waterflooded** yes

**Brine Analysis**

**Brine sample number** EOR-B28

**Temperature (C)** 25

**Resistivity** 0.155 ohm-m

**Eh (mV)** -271

**pH** 6.9

**Anion chemistry (mg/L)**

Br	<1	I	<1
Cl	23750	NH <sub>4</sub>	112
CO <sub>3</sub>	290	NO <sub>3</sub>	87
HCO <sub>3</sub>	<1	SO <sub>4</sub>	<1

**Cation chemistry (mg/L)**

Al	1.45	Co	<0.05	Mo	<0.05	Si	5.1
As	2.4	Cr	0.44	Na	17650	Sr	92
B	2.97	Cu	0.11	Ni	<0.15	Ti	0.09
Ba	140	Fe	0.25	Pb	<0.4	V	0.30
Be	0.0	K	70	Rb	<10	Zn	0.02
Ca	935	Mg	545	Sb	<0.3	Zr	0.05
Cd	<0.05	Mn	0.25	Se	1.8		



**APPENDIX A** *continued*

**API Number** 1202701127

**Operator** Robben

**Well Name** Kormann No. 5

**Location** SW NE SE, Sec. 5, T1N-R3W

**Perforations Depth** 979.5-980.5 ft Cypress red interval

**Surface Elevation** not reported

**Waterflooded** yes, presently inactive

**Brine Analysis**

**Brine sample number** EOR-B29

**Temperature (C)** 25

**Resistivity** 0.168 ohm-m

**Eh (mV)** -275

**pH** 7.2

**Anion chemistry (mg/L)**

Br	<1	I	<1
Cl	28850	NH <sub>4</sub>	164
CO <sub>3</sub>	172	NO <sub>3</sub>	128
HCO <sub>3</sub>	<1	SO <sub>4</sub>	<1

**Cation chemistry (mg/L)**

Al	1.45	Co	<0.05	Mo	<0.05	Si	4.65
As	1.8	Cr	0.53	Na	18000	Sr	92
B	2.62	Cu	0.11	Ni	<0.15	Ti	0.09
Ba	3.15	Fe	0.2	Pb	<0.4	V	0.30
Be	0.0	K	70	Rb	<10	Zn	<0.02
Ca	980	Mg	585	Sb	<0.3	Zr	0.05
Cd	<0.05	Mn	0.33	Se	1.8		

**APPENDIX A** *continued*

**API Number** 1202701106

**Operator** Robben

**Well Name** Schlarmann No. 3

**Location** NW SE SE, Sec. 5, T1N-R3W

**Perforations Depth** 973-974 ft Cypress red interval

**Surface Elevation** not reported

**Waterflooded** yes, presently inactive

**Brine Analysis**

**Brine sample number** EOR-B30

**Temperature (C)** 25

**Resistivity** 0.175 ohm-m

**Eh (mV)** -120

**pH** 7.08

**Anion chemistry (mg/L)**

Br	<1	I	<1
Cl	29915	NH <sub>4</sub>	192
CO <sub>3</sub>	258	NO <sub>3</sub>	149
HCO <sub>3</sub>	<1	SO <sub>4</sub>	<1

**Cation chemistry (mg/L)**

Al	1.35	Co	<0.05	Mo	<0.05	Si	6.1
As	1.9	Cr	0.44	Na	16850	Sr	92
B	3.22	Cu	0.1	Ni	<0.15	Ti	0.09
Ba	32.4	Fe	21.6	Pb	<0.4	V	0.30
Be	0.0	K	70	Rb	<10	Zn	<0.02
Ca	935	Mg	550	Sb	<0.3	Zr	0.05
Cd	<0.05	Mn	0.48	Se	1.3		

**APPENDIX A** *continued*

**API Number** 1202701105

**Operator** Robben

**Well Name** Schlarmann 0-4

**Location** NE SE SE, Sec. 5, T1N-R3W

**Perforations Depth** 978.5-979 ft Cypress red interval

**Surface Elevation** not reported

**Waterflooded** yes, presently inactive

**Brine Analysis**

**Brine sample number** EOR-B31

**Temperature (C)** 25

**Resistivity** 0.158 ohm-m

**Eh (mV)** -338

**pH** 6.87

**Anion chemistry (mg/L)**

Br	<1	I	<1
Cl	25135	NH <sub>4</sub>	175
CO <sub>3</sub>	416	NO <sub>3</sub>	136
HCO <sub>3</sub>	<1	SO <sub>4</sub>	<1

**Cation chemistry (mg/L)**

Al	1.45	Co	<0.05	Mo	<0.05	Si	5.35
As	2.3	Cr	0.42	Na	18550	Sr	97
B	3.43	Cu	0.1	Ni	<0.15	Ti	0.09
Ba	92	Fe	0.25	Pb	<0.4	V	0.30
Be	0.0	K	70	Rb	<10	Zn	<0.02
Ca	995	Mg	590	Sb	<0.3	Zr	0.05
Cd	<0.05	Mn	0.18	Se	1.2		

**APPENDIX A** *continued*

**API Number** 1202701560

**Operator** H.S. Woodard Sr.

**Well Name** Trame No. 1

**Location** NE NE NW, Sec. 8, T1N-R3W

**Perforations Depth** 955-990 ft Cypress red interval

**Surface Elevation** 472 ft (Kelly bushing)

**Waterflooded** yes, presently inactive

**Brine Analysis**

**Brine sample number** EOR-B18

**Temperature (C)** 25

**Resistivity** 0.165

**Eh (mV)** -197

**pH** 7.05

**Anion chemistry (mg/L)**

Br	I		
Cl 35000	NH <sub>4</sub> 150		
CO <sub>3</sub>	NO <sub>3</sub> 116		
HCO <sub>3</sub> 232	SO <sub>4</sub>		

**Cation chemistry (mg/L)**

Al 1.33	Co <0.07	Mo <0.08	Si 3.90
As 2.8	Cr 0.48	Na 17870	Sr 96
B 2.87	Cu <0.06	Ni <0.15	Ti 0.07
Ba 65.4	Fe 6.41	Pb <0.4	V 0.29
Be 0.0018	K 62	Rb <10	Zn <0.02
Ca 936	Mg 556	Sb 1.3	Zr 0.05
Cd <0.05	Mn 0.8	Se 1.5	

**APPENDIX A** *continued*

**API Number** 1202724590

**Operator** Oelze

**Well Name** Robben No. 1

**Location** SE SW SE, Sec. 5, T1N-R3W

**Perforations Depth** 966-970 ft; 999-1003 ft Cypress red interval

**Surface Elevation** 472 ft (Kelly bushing)

**Waterflooded** yes, presently inactive

**Oil Analysis**

**Oil sample number** EOR-69

***Hydrocarbon fraction (%)***

saturated hydrocarbons 74.91

aromatic hydrocarbons 18.15

resins 5.60

asphaltenes 1.34

***Selected hydrocarbon ratios***

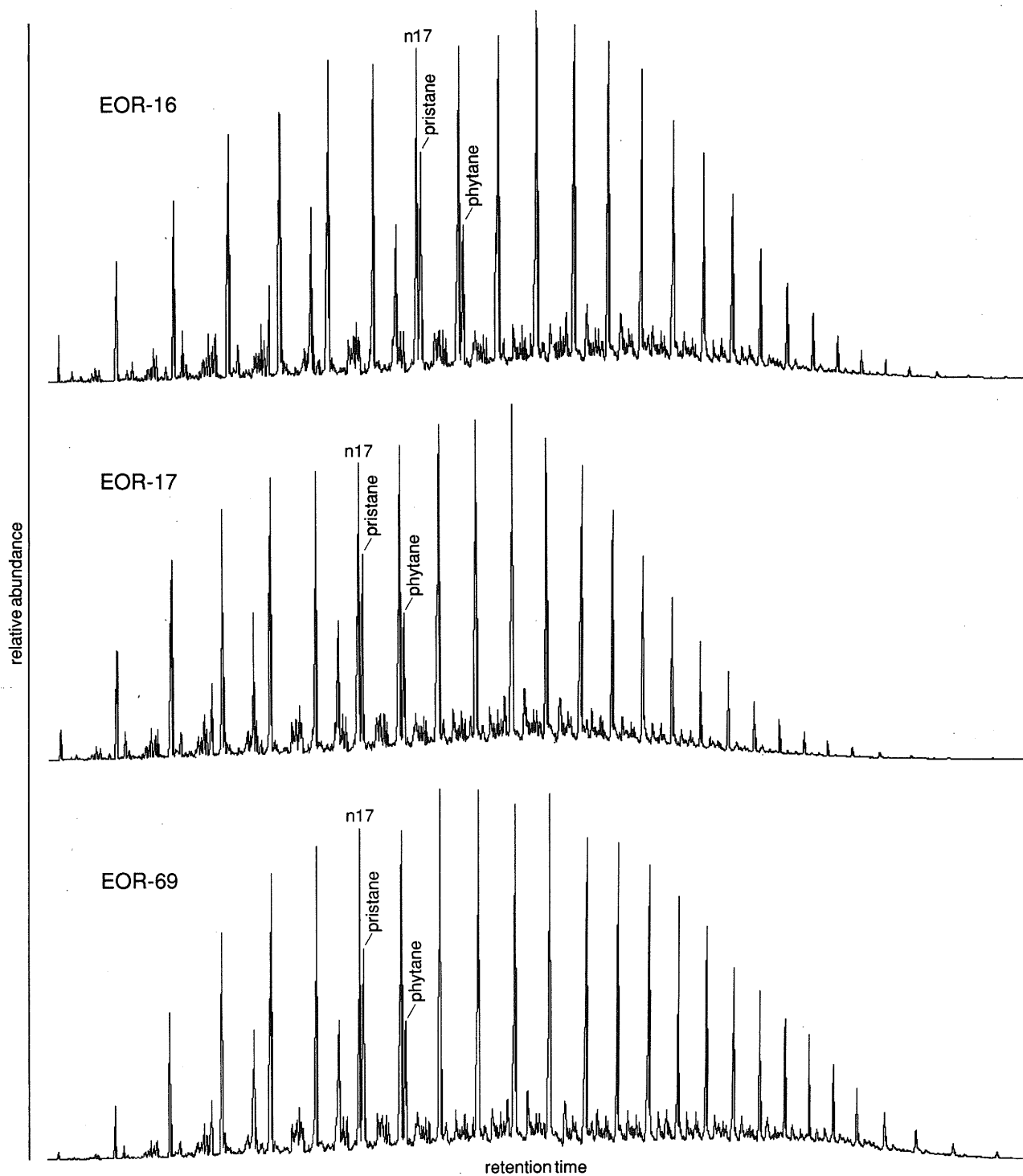
C17/C18 0.983

pristane/phytane 2.613

pristane/C17 1.350

phytane/C18 3.589

# APPENDIX B GAS CHROMATOGRAMS OF SATURATED HYDROCARBONS



## APPENDIX C CYPRESS RESERVOIR SUMMARY

**Field** Bartelso

**Location** Clinton County, Illinois; Secs. 4, 5, 8, and 9, T1N-R3W

**Tectonic/Regional Setting** intracratonic basin

**Geologic Structure** drape over a Silurian pinnacle reef

**Trap Type** structural/stratigraphic

**Reservoir Drive** gas dissolution

**Original Reservoir Pressure** NA

### Reservoir Rocks

**Age** Mississippian (Chesterian)

**Stratigraphic unit** Cypress

**Lithology** quartz arenite-subarkose

**Wetting characteristics** red interval, oil-wet; all other intervals water-wet

**Depositional environments** red interval, tidal shoal/tidal bar; gray interval, delta plain to lagoonal; purple interval, upper shoreface; pink interval, delta front/delta fringe

**Productive facies** sandstones of the red, gray, and purple intervals

**Petrophysics** ( $\phi$  and  $k$  from unstressed conventional core;  $S_w$  from logs)

**Porosity Type:** ( $\phi$  total 20%: primary 15%; secondary 5%)

	Average	Range	Cutoff
$\phi$	20%	16–26%	16%
$k$ air (md)	200	16–620	100
$k$ liquid	NA	NA	NA
$S_w$	30%	10–95%	50%
$S_{or}$	70%	5–90%	50%
$S_{gr}$	NA	NA	NA
<i>Cementation factor</i>	NA	NA	NA

### Source Rocks

**Lithology and stratigraphic unit** shale; New Albany Group

**Time of hydrocarbon maturation** Permo-Triassic

**Time of trap formation** Chesterian (stratigraphic); Penn./Perm. (structural)

### Reservoir Dimensions

**Depth** 970–1100 ft

**Areal dimensions** 560 acres

**Productive area** 440 acres

**Number of pay zones** 3

**Hydrocarbon column** 70 ft

**Initial fluid contacts** gas/oil, -492 ft; oil/water, -550 ft (purple); -540 ft (gray)

**Average net sand thickness** red 'A' interval, 4 ft; red 'B' interval, 4 ft; gray interval, 2 ft; purple interval, 6 ft

**Average gross sand thickness** red 'A' interval, 5 ft; red 'B' interval, 6 ft; gray interval, 4 ft; purple interval, 8 ft

**Net/gross** red 'A', 4/5; red 'B', 4/6; gray, 2/4; purple, 6/8

**Initial reservoir temperature** 100°F (estimated from logs)

**Fractured** natural, NA; artificial, nitroglycerin induced

### Wells

**Spacing** 10-acre primary; no spacing on waterflood

**Pattern** normal primary with 5-spot injection program

**Total** 136 (producers 43; water source 2; observation 0; suspended 0; injection 24; disposal 3; abandoned 37; dry holes 27)

**Reservoir Fluid Properties**

**Hydrocarbons**

*Type* oil and gas  
*GOR* NA  
*API gravity* 36°  
*FVF* 1.15  
*Viscosity* 6.3 cp @ 71°F  
*Bubble point pressure* NA

**Formation water**

*Resistivity* 0.16 @ 77°F  
*Total dissolved solids* 55,000 ppm

**Volumetrics**

**In-place** 5,062,000 BBLs STOOIP  
**Cumulative production** 2.5 MMBO  
**Ultimate recovery**  
*Primary* 1.25 MMBO  
*Secondary* 1.25 MMBO  
*Tertiary* NA  
**Recovery efficiency**  
*Primary* 25%  
*Secondary* 25%  
*Tertiary* NA

**Typical Drilling/Completion/Production Practices**

**Completions** open hole or cased  
**Drilling fluid** fresh water mud  
**Fracture treatment** 20–40 quarts of nitroglycerin  
**Acidization** none  
**Producing mechanism**  
*Primary* pump  
*Secondary* pump

**Typical Well Production (to date)**

**Average daily IP** 74 BOPD (red interval); 27 BOPD (gray interval); 66 BOPD (purple interval); 80 BOPD (commingled)  
**Cumulative production** 33,000 BO (primary and secondary)  
**Water/oil ratio (initial)** NA



## ERRATA

1992

Illinois Petroleum 137

Illinois State Geological Survey

***Reservoir Heterogeneity and Potential for  
Improved Oil Recovery within the Cypress Formation  
at Bartelso Field, Clinton County, Illinois***

Stephen T. Whitaker and Andrew K. Finley

Page 21, paragraph 6, last line:

*for* Minor shifts in the

*read* Minor shifts in the clastic influx and/or changes in marine currents would account for the shingled nature of the bars.